fib CEB-FIP
PCI Precast/Prestressed Concrete Institute

Bulletin 94

Precast concrete bridge continuity over piers

Technical report

Bulletin 94

fib CEB-FIP

PCI Precast/Prestressed Concrete Institute

Precast concrete bridge continuity over piers

Technical Report

Task Group 6.5

July 2020

Approval for this bulletin

Subject to priorities defined by the Technical Council and the Presidium, the results of the *fib*'s work in commissions and task groups are published in a continuously numbered series of technical publications called *bulletins*. The following categories are used:

Category:	**Approval by**:
Technical report	Task group and chairpersons of the commission
State-of-the-art report	Commission
Manual / Guide to good practice / Recommendation	Technical Council
Model code	General Assembly

Any publication not having met the above requirements will be clearly identified as a preliminary draft.

fib Bulletin 94 was approved as a technical report by Commission 6 *Prefabrication* in 2020.

Maher Tadros (convener and editor; e.Construct, USA)

Hugo Corres Peiretti (convener and editor; FHECOR Ingenieros Consultores, Spain)

Freddy Ariñez Fernandez (Universidad Politécnica de Madrid, Spain), Chen Baochun (Fuzhou University, China), Andre de Chefdebien (LB7, France), Albert de la Fuente Antequera (Universidad Politécnica de Cataluña, Spain), Sameh El-Ashri (eConstruct, UAE), David Fernandez-Ordoñez (the *fib*, Switzerland), Helder Figueiredo (IDEAM, Spain), Mario Garcia Gonzalez (Pacadar, Spain), Pankaj Garg (Atkins, India), Man Yop Han (Asian Concrete Federation, South Korea), Milan Kalny (Pontex s.r.o., Czech Republic), Kenichi Kata (Sumitomo Mitsui, Japan), Byung Suk Kim (Hanyang University), Lars Lundorf Nielsen (COWI, Denmark), Luis Matute Rubio (IDEAM, Spain), William Nickas (PCI – Precast/Prestressed Concrete Institute, USA), Alessandro Palermo (University of Canterbury, Italy/New Zealand), Sung Yong Park (KICT, South Korea), Mario Petrangeli (Mario Petrangeli & Associati, Italy), Ruslan Pogrebnyak (Russia), Jong Sung Sim (Hanyang University, South Korea), Fernando Stucchi (EGT Engenharia, Brazil), Jasson Tan (Dura Technology, Malaysia), Pieter van der Zee (Ergon, Belgium), Yen Lei Voo (Dura Technology, Malaysia), Marcelo Waimberg (EGT Engenharia, Brazil), Robert Wheatley (Atkins, UK), and Wen Chan Yin (National Taiwan University, Taiwan).

Cover image: Bridge on I-80 near Omaha, Nebraska, USA

ISSN 1562-3610
ISBN 978-2-88394-140-3
https://doi.org/10.35789/fib.BULL.0094
Layout by Marie Reymond (*fib*).
Printed by DCC Document Competence Center Siegmar Kästl e.K., Germany

Acknowledgements

This report was drafted by Task Group 6.5 "Precast concrete bridges" within the *fib* Commission 6.

Authors:

Maher Tadros (Convener/Editor)
e.Construct, USA

Hugo Corres Peiretti (Convener/Editor)
Technical University of Madrid, Spain

Athul Alex
e.Construct, USA

Andre de Chefdebien
LB7, France

David Fernández-Ordóñez
The *fib*, Switzerland

Mario García
Pacadar, Spain

Luis Matute
IDEAM, Spain

William Nickas
PCI, USA

Borja Regúlez
FHECOR, Spain

Pieter van der Zee
Ergon, Belgium

Robert Wheatley
Atkins, UK

Freddy Aríñez
FHECOR, Spain

Mamdouh El-Badry
University of Calgary, Canada

Helder Figueiredo
IDEAM, Spain

Amgad Girgis
e.Construct, USA

Gonzalo Navarro
FHECOR, Spain

Mario Petrangeli
Mario Petrangeli & Associati, Italy

Fernando Stucchi
EGT, Brazil

Marcelo Waimberg
EGT, Brazil

Contact details of Task Group members can be found in the members only section of the *fib* website, www.fib-international.org.

Authors by chapter

Chapters	Main authors
1	Alex, Aríñez, Corres, El-Badry, Fernández-Ordóñez, García, Navarro, Petrangeli, Regúlez, Stucchi, Tadros, van der Zee, Waimberg, and Wheatley
2	Alex, Aríñez, Corres, El-Badry, Fernández-Ordóñez, García, Navarro, Petrangeli, Regúlez, Stucchi, Tadros, van der Zee, Waimberg, and Wheatley
3	Alex, Aríñez, Corres, El-Badry, Fernández-Ordóñez, García, Navarro, Petrangeli, Regúlez, Stucchi, Tadros, van der Zee, Waimberg, and Wheatley
4	Alex, Aríñez, Corres, El-Badry, Fernández-Ordóñez, García, Navarro, Petrangeli, Regúlez, Stucchi, Tadros, van der Zee, Waimberg, and Wheatley
5	Alex, Aríñez, Corres, El-Badry, Fernández-Ordóñez, García, Navarro, Petrangeli, Regúlez, Stucchi, Tadros, van der Zee, Waimberg, and Wheatley
6	Alex, Aríñez, Corres, El-Badry, Fernández-Ordóñez, García, Navarro, Petrangeli, Regúlez, Stucchi, Tadros, van der Zee, Waimberg, and Wheatley
7	Alex, Aríñez, Corres, El-Badry, Fernández-Ordóñez, García, Navarro, Petrangeli, Regúlez, Stucchi, Tadros, van der Zee, Waimberg, and Wheatley
8	Alex, Aríñez, Corres, El-Badry, Fernández-Ordóñez, García, Navarro, Petrangeli, Regúlez, Stucchi, Tadros, van der Zee, Waimberg, and Wheatley
9	de Chefdebien, Figueiredo, Girgis, Matute, Nickas, Tadros
10	Aríñez, Corres, Navarro, Regúlez, Tadros
11	Aríñez, Corres, Navarro, Regúlez, Tadros

Preface

Concrete bridges are an important part of today's road infrastructure. An important part of those concrete bridges is to a large extent prefabricated. Precast concrete enables all the advantages of an industrialized process to be fully utilized. Contemporary concrete mixtures are used to realize high-strength bridge girders and piers that exactly meet the requirements set, both structurally and aesthetically, with a small ecological footprint. Sustainable and durable! On the construction site, there is no need for complex formwork, the execution time is drastically reduced and where road, water and rail traffic on or under the bridge has to be temporarily interrupted, it is only minimally inconvenienced during the execution of the project.

There is a wide variety of prefabricated bridges. In 2004, the *fib* commission on prefabrication already published the Bulletin 29 *Precast concrete bridges* which, in addition to the history of prefabricated bridges, also gave an overview of the different bridge types and structural systems. This document elaborates on one specific structural system: the continuous bridge. Task Group 6.5 "Precast concrete bridges" discusses in detail how to achieve continuity over the piers with precast elements. This bulletin bundles the experiences of experts in the field of bridge design so that less experienced designers would be able to identify the points of attention and make a correct design. In addition to the theoretical considerations, the principles are tested against three realizations in the USA and Europe.

Commission 6 thanks the Co-Conveners Maher Tadros and Hugo Corres and all active members of the Task Group for sharing their knowledge and experience and for the successful realization of this bulletin.

Stef Maas
Chair of the Commission 6: *Prefabrication*

Harry Gleich
Chair of PCI Technical Activities Council

Contents

1. Introduction

Bridges that consist of simple-span precast concrete beams made continuous after the deck weight is introduced are also known as continuous for live load bridges.

The beams carry their own dead load and the slab dead load as simple spans, but all the subsequent loads are carried as continuous spans. Deck reinforcement provides the negative moment resistance. If net camber due to simple-span loads (girder weight, prestress, and deck weight) is upward, a positive moment develops, and the connection could crack. For this reason, positive moment reinforcement at the joint over the piers is required. Positive moment cracking should be considered in design for negative moment. Cracking may limit negative moment transfer until the cracks close.

This chapter was mainly authored by Alex, Aríñez, Corres, El-Badry, Fernández-Ordóñez, García, Navarro, Petrangeli, Regúlez, Stucchi, Tadros, van der Zee, Waimberg, and Wheatley.

https://doi.org/10.35789/fib.BULL.0094.Ch01

2. Scope

The purpose of this document is to carry out a phenomenological study of the evolution of the restraint moment over piers, as well as to describe a simplified methodology that can easily estimate its value.

In addition, this document presents some examples using the proposed methodology developed according the traditions of different countries.

This document is aimed at engineers without experience because it establishes the subject of continuity of precast concrete superstructures in a clear and concise manner. It is also aimed at experienced engineers, because it uses examples to show the procedures and simplifications used in different countries.

This chapter was mainly authored by Alex, Aríñez, Corres, El-Badry, Fernández-Ordóñez, García, Navarro, Petrangeli, Regúlez, Stucchi, Tadros, van der Zee, Waimberg, and Wheatley.
https://doi.org/10.35789/fib.BULL.0094.Ch02

3. Notation

This document uses the *fib* Model Code 2010 notations shown below. The notation used by the American Association of State Highway and Transportation Officials' AASHTO LRFD Bridge Design Specifications is shown in brackets in the cases where it is different.

A_B = area of cross section of precast concrete beam
$A_h^{"2"}$ = area of cross section of composite section for gradually developing stress
A_S = area of cross section of cast-in-place top slab
$E_B(t)$ = modulus of elasticity of girder at time t
$E_C(t)$ = modulus of elasticity of concrete at time t
$E_{C,\varphi}$ = reference modulus of elasticity for creep calculation
$E^*_{ctc}(t,t_0)$ = effective modulus of elasticity for constant sustained stress
$E^*_{ctv}(t,t_0)$ = effective modulus of elasticity for gradually developing stress
$E_S(t)$ = modulus of elasticity of deck at time t
I_B = moment of inertia of precast concrete beam
$I_h^{"2"}$ = moment of inertia of composite section for gradually developing stress
I_S = moment of inertia of cast-in-place top slab
L_1 = length of span 1
L_2 = length of span 2
M_{B+S} = bending moment on composite section
M_{ext} = external bending moment
M_{int} = internal bending moment
M_{sh} = bending moment due to free shrinkage
N_{B+S} = normal force on composite section
N_{ext} = external normal force
N_{int} = internal normal force
N_{sh} = axial force due to free shrinkage
δ = redistribution coefficient
$\Delta\theta^{left}$ = rotation at left of support
$\Delta\theta^{left}_{elastic}$ = elastic rotation at left of support
$\Delta\theta^{right}$ = rotation at right of support
$\Delta\theta^{right}_{elastic}$ = elastic rotation at right of support
$\varepsilon(t)$ = strain
E_{B+S} = composite girder + deck strain
$\varepsilon_{cr}(t)$ = time-dependent creep strain
$\varepsilon_{sh}(t)$ = free shrinkage strain
θ = rotation at support
$\sigma(t)$ = stress applied at time t
$\varphi(t,t_0)$ = creep coefficient at time t for concrete loaded at time t_0 [$\psi(t,t_0)$]
$\varphi_B(t,t_0)$ = creep coefficient of girder between initial time of loading t_0 and final time [$\psi_B(t,t_0)$]
$\varphi_S(t,t_0)$ = creep coefficient of deck between initial time of loading t_0 and final time [$\varphi_S(t,t_0)$]
$\chi(t,t_0)$ = aging coefficient

This chapter was mainly authored by Alex, Aríñez, Corres, El-Badry, Fernández-Ordóñez, García, Navarro, Petrangeli, Regúlez, Stucchi, Tadros, van der Zee, Waimberg, and Wheatley.
https://doi.org/10.35789/fib.BULL.0094.Ch03

4. Phenomenological study of restraint moments over the piers

Creep analysis for positive restraint moments over the piers has been studied in detail[4-1, 4-2, 4-3, 4-4, 4-5, 4-6, 4-7, 4-8, 4-9, 4-10]. In general, creep of the beam under the net effects of prestressing, self-weight, deck weight, and superimposed dead loads will tend to produce additional upward camber with time. Shrinkage of the deck concrete will tend to produce downward camber of the composite system with time. In addition, loss of prestress due to creep, shrinkage, and relaxation will result in downward camber. Depending on the properties of the concrete materials and the age at which the beams are erected and subsequently made continuous, either positive or negative moments may occur over continuous supports.

In situations where beams are made continuous at a relatively young age, it is more likely that positive moments will develop with time at the supports. These positive restraint moments are the result of the tendency of the beams to continue to camber upwards because of ongoing creep strains associated with the prestressing forces. Shrinkage of the deck concrete, loss of prestress, and creep strains due to self-weight, deck weight, and superimposed dead loads all tend to reduce this positive moment.

When beams are mature when they are made continuous, negative moments at the supports could result. This is especially true when the beams have short spans and large depths, thus requiring relatively low prestress levels. In these conditions, the time-dependent creep strains associated with prestress have diminished to the point that the creep effects that produce downward deflection (beam weight and deck weight) are larger. This will induce negative restraint moments at the supports.

The effects of diaphragm cracking on bridge performance due to positive moments continue to be a hotly debated subject. An argument can be made[4-11] that continuity for live loads becomes unreliable after a small crack has opened near the bottom of the diaphragm. It is pointed out that a finite end rotation is required to close this crack, forcing the beam to carry live loads as a simple-span member. Theoretically, this simple-span action results in live load moments that are significantly higher than those predicted by calculations that assume full continuity.

Countering this argument, however, is the successful experience of the many countries and agencies that routinely design precast, prestressed concrete bridges under the assumption of full continuity for live loads. One study[4-10] showed that the diaphragm crack needs to be larger than 0.012 inch (0.3 mm) before negative moment transfer is lost. Cracking at the bottom fibers of the midspan region of these bridges due to design for smaller live load moment in the continuous-span scenario has not been reported. In addition, only service load behavior is significantly affected. Under ultimate limit state (ULS) loads, end rotations of the beams will be large enough to close any crack that may have opened at the piers, restoring full continuity. It should be agreeable, therefore, that ultimate capacity is unaffected by existence of controlled bottom cracks in the beams at the pier areas.

This chapter was mainly authored by Alex, Aríñez, Corres, El-Badry, Fernández-Ordóñez, García, Navarro, Petrangeli, Regúlez, Stucchi, Tadros, van der Zee, Waimberg, and Wheatley.
https://doi.org/10.35789/fib.BULL.0094.Ch04

5. Long-term constitutive equations (aging factor approach)

The following sections describe a procedure that can be used to carry out time-dependent analysis of any type of composite prestressed concrete bridge. This method is based on traditional composite section analysis, using transformed elastic properties to reflect creep characteristics. So-called initial strains are introduced in the analysis to account for the effects of member restraint due to concrete creep.

5.1 Stress-strain-time relationship

The stress-strain-time relationship for the concrete material will predict the total strain ε at a future time t, which results from a stress increment applied at time t_0. The total concrete strain at any time t can be separated into three components:

ε_σ: immediate strain due to the applied stress σ

ε_{cr}: time-dependent creep strain

ε_{sh}: free shrinkage strain

It is important to recognize that both the modulus of elasticity E and the creep coefficient φ are functions of time. In addition, because concrete is an aging material, φ also depends on the loading age t_0.

5.2 Constant stress

Total concrete strain ($\varepsilon_\sigma + \varepsilon_{cr}$) is usually expressed as follows:

$$\varepsilon(t) = \frac{\sigma}{E_c\left(t_0\right)} + \frac{\sigma}{E_{c,\varphi}}\varphi\left(t,t_0\right) \tag{5-1}$$

where:

- $E_c(t_0)$ is the modulus of elasticity of concrete at time t_0, the beginning of the interval being considered
- $E_{c\varphi}$ is the reference modulus of elasticity for creep calculation
- $\varphi(t,t_0)$ is the creep coefficient during a time interval from t_0 to t for stress applied at time t_0 and kept constant

This equation applies as long as the stress s is a constant, sustained stress.

Figure 5-1 shows gradual development of creep strain, associated with constant stress, with time.

This chapter was mainly authored by Alex, Aríñez, Corres, El-Badry, Fernández-Ordóñez, García, Navarro, Petrangeli, Regúlez, Stucchi, Tadros, van der Zee, Waimberg, and Wheatley.

https://doi.org/10.35789/fib.BULL.0094.Ch05

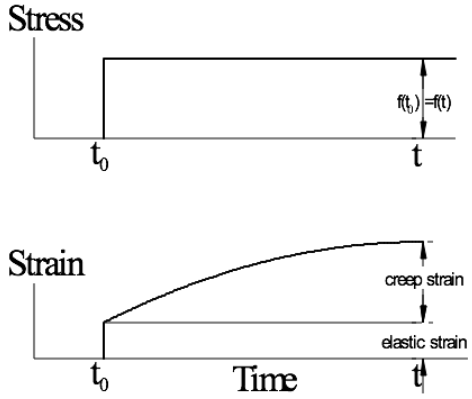

Fig. 5-1 Time versus concrete strain under constant stress, shrinkage is excluded

Some publications[5-1, 5-2, 5-3] recommend simplifying Eq. (5-1), assuming $E_{c\varphi}$ is equal to $E_c(t_0)$. With this simplification, we obtain Eq. (5-2):

$$\varepsilon(t) = \frac{\sigma(t_0)}{E_c(t_0)}\left[1+\varphi(t,t_0)\right] \tag{5-2}$$

5.3 Variable Stress

When the applied stress σ is variable, Eq. (5-2) cannot be directly used.

Figure 5-2 depicts the development of creep strain under the effect of a gradually introduced stress. Using the principle of superposition, the effects of a series of applied stress increments can be determined individually, using Eq. (5-1), and then combined to calculate the total time-dependent concrete strain. This approach is often called time-step method and is suitable for numerical computer modeling.

Another approach is called the age-adjusted effective modulus method. In this method, an "aging factor" is applied to the creep coefficient to account for the effect that the stress is gradually introduced to an aging concrete with gradually increasing modulus of elasticity and decreasing creep effect[5-4, 5-5]. The aging coefficient $\chi(t,t_0)$ is a function of age of concrete at time of initial load introduction and a number of other factors. The total strain is represented by Eq. (5-3):

$$\varepsilon(t) = \frac{\sigma(t)}{E_{c,0}} + \chi(t,t_0)\frac{\sigma(t)}{E_{c,\varphi}}\varphi(t,t_0) \tag{5-3}$$

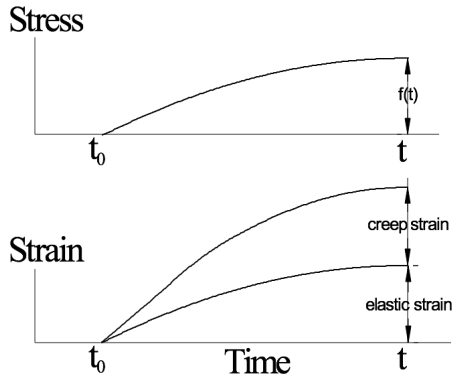

Fig. 5-2 Time versus concrete strain under variable stress, shrinkage excluded

As in the previous case, Eq. (5-4) can be simplified into the following expression:

$$\varepsilon(t) = \frac{\sigma(t)}{E_c(t_0)}\left[1 + \chi(t,t_0)\varphi(t,t_0)\right] \tag{5-4}$$

5.4 Effective elastic modulus

A pseudo-elastic analysis can be carried out by assuming a reduced modulus of elasticity that accounts for creep effects. The age-adjusted effective modulus of elasticity of concrete is defined as follows:

For constant sustained stress:

$$E^*_{ctc}(t,t_0) = \frac{E_c(t_0)}{1+\varphi(t,t_0)} \tag{5-5}$$

For gradually developing stress, the age-adjusted effective modulus is:

$$E^*_{ctv}(t,t_0) = \frac{E_c(t_0)}{1+\chi(t,t_0)\varphi(t,t_0)} \tag{5-6}$$

The mathematical expression of the creep function is an approximation that was developed from experimental results. There are different formulations defined in the different references and codes[5-1, 5-6, 5-7, 5-8] and, generally, they show important differences. Engineers often use these formulas in their design. However, during construction it is possible to use experimental results to adjust the creep function to reflect the characteristics of the concrete used on site[5-1, 5-6].

The expression that represents the evolution, over time, of the modulus of elasticity is another characteristic that is usually estimated from available experimental results.

6. Estimation of the continuity forces

The detailed pseudo-elastic analysis is generally done using full uncracked concrete section properties. It does not account for loss of stiffness due to cracking, which can create considerable relief of the calculated restraint moment. In some countries, a reduction factor of 0.9 is applied to the uncracked section restraint moment.

On one hand, loads applied before continuity is made create creep restraint moments in the continuous beam. On the other hand, loads introduced after the beam becomes continuous only create elastic (no-creep) moments.

The analysis is made for a continuous beam with rigid vertical supports while allowing the beam to rotate and to translate horizontally over the supports. Only one support is fixed against horizontal translation to maintain stability. With these assumptions, uniform shrinkage and temperature change only induce axial deformation and do not induce curvature or flexure.

The analysis, using pseudo-elastic properties, allows for superposition of various effects.

As shown in Sections 6.1-6.3, the analysis is given for each of the following effects separately and then superimposed to create the net effect. These effects are: prestress (including prestress losses), girder self-weight, deck self-weight, superimposed dead loads (barriers and overlays), differential shrinkage, and temperature gradient.

To simplify the analysis, the following assumptions have been adopted:

- $E_{c,\varphi}$ is equal to $E_c(t_0)$.
- Concrete of the top slab hardens at the same time that continuity is made.

6.1 Restraint moments due to creep

6.1.1 Girder self-weight, prestressing, and slab self-weight

In this section, the pseudo-elastic analysis is developed for loads that are introduced before continuity is made: girder self-weight, prestressing, and top slab self-weight.

6.1.1.1 Application on simply supported girder (t_0)

The previously described loads produce axial forces N_{ext} and bending moments M_{ext} in each section of the girder. The resulting strains and curvatures in each section can be determined with Eq. (6-1) and (6-2):

$$\varepsilon_B(t_0) = \frac{N_{ext}}{A_B \cdot E_B(t_0)} \tag{6-1}$$

$$\chi_B(t_0) = \frac{M_{ext}}{I_B \cdot E_B(t_0)} \tag{6-2}$$

This chapter was mainly authored by Alex, Aríñez, Corres, El-Badry, Fernández-Ordóñez, García, Navarro, Petrangeli, Regúlez, Stucchi, Tadros, van der Zee, Waimberg, and Wheatley.

https://doi.org/10.35789/fib.BULL.0094.Ch06

6.1.1.2 Hardening of the top slab and continuity over the piers (t_1)

From time t_0 to time t_1, the strains and curvatures of the different girder sections evolve according to the creep laws given in Eq. (6-3) and (6-4):

$$\varepsilon_B(t_1) = \frac{N_{ext}}{A_B \cdot E_B(t_0)}\left[1+\varphi_B(t_1,t_0)\right] \tag{6-3}$$

$$\chi_B(t_1) = \frac{M_{ext}}{I_B \cdot E_B(t_0)}\left[1+\varphi_B(t_1,t_0)\right] \tag{6-4}$$

6.1.1.3 Evaluation at a time infinity (t)

The hardening of the top slab and the onset of continuity result in two statically indeterminate compatibilities that influence the strains and curvatures of the different sections of the structure.

On one hand, if we neglect the existence of the top slab and the continuity between the girders, the different sections of the girder would experience a strain and curvature increase due to creep from time t_1 to time t.

However, the top slab and the continuity restrain these strains and curvatures. Consequently, the strains and curvatures of the composite section (girder + slab) are different than the ones experienced only by the girder.

First, the calculation of the rotations of the girder + slab system is made without considering the continuity over the piers. To determine this, the general calculation method for composite sections can be used.

- Determine the strains and curvatures of the girder, releasing the structure from the influence of the top slab and the continuity.

$$\Delta\varepsilon_B(t,t_1) = \frac{N_{ext}}{A_B \cdot E_B(t_0)}\left[\varphi_B(t,t_0)-\varphi_B(t_1,t_0)\right] \tag{6-5}$$

$$\Delta\chi_B(t,t_1) = \frac{M_{ext}}{I_B \cdot E_B(t_0)}\left[\varphi_B(t,t_0)-\varphi_B(t_1,t_0)\right] \tag{6-6}$$

Apply normal forces and moments on the girder that compensate these deformations.

$$N_{\text{int}} = -\Delta\varepsilon_B(t_n,t_1)\frac{E_B(t_1)}{1+\chi\cdot\varphi_B(t_n,t_1)}A_B \tag{6-7}$$

$$M_{\text{int}} = -\Delta\chi_B(t_n,t_1)\frac{E_B(t_1)}{1+\chi\cdot\varphi_B(t_n,t_1)}I_B \tag{6-8}$$

$$N_{\text{int}} = N_{ext}\frac{E_B(t_1)}{E_B(t_0)}\frac{\varphi_B(t_n,t_0)-\varphi_B(t_1,t_0)}{1+\chi\cdot\varphi_B(t_n,t_1)} \tag{6-9}$$

$$M_{\text{int}} = N_{ext}\frac{E_B(t_1)}{E_B(t_0)}\frac{\varphi_B(t_n,t_0)-\varphi_B(t_1,t_0)}{1+\chi\cdot\varphi_B(t_n,t_1)} \tag{6-10}$$

- Apply the opposite values of these forces and moments on the composite section. The composite section should be transformed by assigning the corresponding effective modulus of elasticity to the girder E_B and to the top slab E_S:

$$E_B = \frac{E_B(t_1)}{1+\chi\cdot\varphi_B(t,t_1)} \tag{6-11}$$

$$E_S = \frac{E_s(t_1)}{1+\chi\cdot\varphi_S(t,t_1)} \tag{6-12}$$

In this document, the mechanical characteristics of the transformed cross section will be noted as $A_h^{"2"}$ and $I_h^{"2"}$.

The forces and moments act on the center of gravity of the transformed cross section. The resulting strains and curvatures in the composite section at time *t* will be the following:

$$N_{B+S} = N_{\text{int}} \tag{6-13}$$

$$M_{B+S} = -M_{\text{int}} - N_{\text{int}}\cdot e \tag{6-14}$$

$$\Delta\varepsilon_{B+S}(t,t_1) = \frac{N_{B+S}}{A_h^{"2"}\cdot E_B(t_1)} = -\frac{N_{ext}}{A_h^{"2"}\cdot E_B(t_0)}\frac{\varphi_B(t,t_0)-\varphi_B(t_1,t_0)}{1+\chi\cdot\varphi_B(t,t_1)} \tag{6-15}$$

$$\Delta\chi_{B+S}(t,t_1) = \frac{M_{B+S}}{I_h^{"2"}\cdot E_B(t_1)} = -\frac{(M_{ext}+N_{ext}\cdot e)}{I_h^{"2"}\cdot E_B(t_0)}\frac{\varphi_B(t,t_0)-\varphi_B(t_1,t_0)}{1+\chi\cdot\varphi_B(t,t_1)} \tag{6-16}$$

We must observe that M_{B+S} is the external moment on the center of gravity of the transformed composite section.

- The net values of the actions in the actual statically indeterminate section are obtained by the summation of the values calculated in the previous steps.

Subsequently, the restraint rotation at the end of the girder can be estimated from the following expression:

$$\Delta\theta = \Delta\theta_{elastic}\frac{E_B(t_1)}{E_B(t_0)}\frac{\varphi_B(t_n,t_0)-\varphi_B(t_1,t_0)}{1+\chi\cdot\varphi_B(t_n,t_1)} \tag{6-17}$$

where $\Delta\theta_{\text{elastic}}$ is the rotation determined instantaneously for the composite beam + slab system with $A_h^{"2"}$ and $I_h^{"2"}$ mechanical characteristics and without the consideration of the continuity over the piers.

The rotations that the composite section tends to develop at both sides of the pier are made compatible with a restraint continuity moment. To determine this moment, a compatible rotation is imposed at time *t*:

$$\Delta\theta^{left} = \Delta\theta^{right} \tag{6-18}$$

$$\begin{aligned}\Delta\theta^{left}_{elastic}\frac{E_B(t_1)}{E_B(t_0)}\frac{\varphi_B(t,t_0)-\varphi_B(t_1,t_0)}{1+\chi\cdot\varphi_B(t,t_1)} - \frac{M\cdot L_1}{3E_B(t_1)I_h^{"2"}} = \\ \Delta\theta^{right}_{elastic}\frac{E_B(t_1)}{E_B(t_0)}\frac{\varphi_B(t,t_0)-\varphi_B(t_1,t_0)}{1+\chi\cdot\varphi_B(t,t_1)} - \frac{M\cdot L_2}{3E_B(t_1)I_h^{"2"}}\end{aligned} \tag{6-19}$$

The compatibility equation for the calculation of a continuous girder, taking into account the mechanical characteristics of the transformed composite section, is:

$$\Delta\theta_{elastic}^{left} - \frac{M \cdot L_1}{3E_B(t_1)I_h^{"0"}} = \Delta\theta_{elastic}^{right} + \frac{M \cdot L_2}{3E_B(t_1)I_h^{"0"}} \tag{6-20}$$

Thus, the restraint moment produced over the piers is equal to the moment determined with a continuous girder analysis taking into account the mechanical characteristics of the transformed composite section multiplied by a constant δ determined with Eq. (6-21):

$$\delta = \frac{E_B(t_1)}{E_B(t_0)} \frac{\varphi_B(t,t_0) - \varphi_B(t_1,t_0)}{1 + \chi \cdot \varphi_B(t,t_1)} \tag{6-21}$$

This coefficient is the same one adopted by different codes and references[6-1, 6-2, 6-3, 6-4] to determine the structural effects of time-dependent behavior of concrete.

6.1.1.4 Steps of the analysis

Determine the moment over the piers with conventional continuous girder analysis.

This moment must be calculated taking into account the transformed composite section with the corresponding effective modulus of elasticity:

$$E_B = \frac{E_B(t_1)}{1 + \chi \cdot \varphi_B(t,t_1)} \tag{6-22}$$

$$E_S = \frac{E_S(t_1)}{1 + \chi \cdot \varphi_S(t,t_1)} \tag{6-23}$$

The restraint moment will then be the moment calculated in the previous step multiplied by the coefficient:

$$\delta = \frac{E_B(t_1)}{E_B(t_0)} \frac{\varphi_B(t,t_0) - \varphi_B(t_1,t_0)}{1 + \chi \cdot \varphi_B(t,t_1)} \tag{6-24}$$

This delta coefficient is a function of the load application time. Therefore, there will be one value for the girder self-weight and prestressing moments and another value for the deck self-weight moments.

6.1.2 Prestress losses

Prestress losses can be considered as an action that evolves over time and in the opposite direction of the applied prestressing force.

If we assume that prestress losses evolve over time proportionally to the creep law, the resulting formulation is analogous to one shown in the previous section, with the exception that it should include the aging coefficient χ.

$$\delta = \frac{E_B(t_1)}{E_B(t_0)} \frac{\chi\left[\varphi_B(t_n,t_0) - \varphi_B(t_1,t_0)\right]}{1 + \chi \cdot \varphi_B(t_n,t_1)} \tag{6-25}$$

6.1.2.1 Steps of the analysis

The steps of the analysis for the prestressing losses are the same as the ones described in section 6.1.1.4, but with the δ coefficient given in Eq. (6-25).

6.2 Effects of deck shrinkage and temperature gradient

6.2.1 Differential shrinkage between the girder and the slab

The procedure used to determine the restraint moment caused by this phenomenon is similar to the evaluation of an incompatible imposed deformation applied to the composite system.

- In each cross section of the bridge, the free deformation of the slab with respect to the girder is allowed.
- Afterwards, an axial load is applied to the slab to restore the compatibility between the girder and the slab.
- The same axial load is applied, but with an opposite sign in the composite system to restore equilibrium. This axial load produces a curvature in each section.
- Because the value of shrinkage is the same in all sections of the bridge, this curvature is constant. From these curvatures, it is possible to calculate the rotations on the ends of the girder. Because this rotation is determined assuming that the girders act as simply supported structures, they are not compatible over the piers and produce a restraint moment that makes them compatible.
- The restraint moment can be determined by introducing at the ends of the continuous bridge, the axial load determined to cancel the deformation of the slab, and the moment product of this axial load and the eccentricity between the center of gravity of the slab and the center of gravity of the composite system with the same mechanical characteristics as in the general example (Eq. (6-26) and (6-27)).

$$N_{sh} = \varepsilon_{sh} \cdot A_S \frac{E_S\left(t_1\right)}{1+\chi \cdot \varphi_S\left(t_n, t_1\right)} \tag{6-26}$$

$$M_{sh} = N_{sh} \cdot Eccentricity \tag{6-27}$$

6.2.1.1 Steps of the analysis

Determine the moment over the piers with conventional continuous girder analysis.

The external actions are an axial load and a moment at the ends of the bridge with the values shown in Eq. (6-26) and (6-27).

This restraint moment must be calculated taking into account the transformed composite section with the effective modulus of elasticity given by Eq. (6-22) and (6-23).

6.2.2 Temperature gradient

Temperature gradients can be assumed as instantaneous actions in time. In general, the temperature gradients proposed by the different codes[6-5, 6-6] are nonlinear along the depth of the cross section.

If the strain distribution is assumed to be linear, in other words a plane cross section is assumed to remain plane after deformation, then nonlinear temperature gradients will result in a state of nonzero self-equilibrating stresses.

6.2.2.1 Steps of the analysis

- Calculate the free strain due to temperature gradient, as $\alpha\Delta T$, at various fibers along the depth of the cross section. This calculation assumes the fibers are free to deform without any restraint.

- Divide the section into layers of similar geometric and material properties. Apply "restraining forces" in these layers to cancel the free strains in the previous step. Each force is equal to the strain times modulus of elasticity times area. The force is a stress resultant and is located at the geometric center of the stress diagram.

- Determine the total moment of the restraining forces about the centroid of the composite section.

- Calculate the curvatures caused by the opposite of the restraining moment (equilibrium).

- The resulting curvatures are introduced in a continuous girder analysis, considering the modulus of elasticity without adjustments, obtaining the restraint moment that compensates the curvature over the piers.

6.3 Superimposed Dead load

The determination of the restraint moment due to the dead load can be solved with an instantaneous general continuous girder analysis.

7. Design of bottom continuity reinforcement

Section 5 of this document discusses methods to estimate the time-dependent restraint positive moment in continuous precast, prestressed concrete bridge beams at the joints over the intermediate supports (piers). In all the previous discussion, analysis is completed using pseudo-elastic analysis with uncracked section properties.

If the positive restraint moment due to the most critical loading combination is less than the moment needed to create flexural cracking at the bottom of the beam at the face of the cast-in-place diaphragm, then no reinforcement would be necessary. However, it is common to expect higher moments than the cracking moment, and therefore flexural cracking.

In this case, two issues emerge: how to use the uncracked member analysis to extrapolate for estimation of the applied moment while the member is cracked, and how to use the applied moment to calculate the required steel reinforcement and to detail it for acceptable serviceability performance. A related issue is how to design the continuous-span beam for negative moment due to full live load effects, considering that it may be cracked over some lengths in the pier regions.

The issues given here have not been fully resolved through research. This explains the wide variety of practices, which rely on experience and engineering judgment. Until research produces better results, the following recommendations are made:

- The restraint moment is calculated using uncracked section analysis. In some codes, a reduction by as much as 10% is allowed to account for reduction due to cracking in the bottom fibers near the pier supports. Although the 10% reduction is quite conservative, it is somewhat consistent with the redistribution allowed for negative moment design.

- Reinforcement is designed using cracked section capacity analysis. In some codes[7-1], a simplified calculation of the steel stress may be used assuming the lever arm between the compression and tension forces is equal to $0.9d$, where d is the effective depth from the compression face to the center of the tensile reinforcement.

- Tensile steel stress is limited to the value obtained from crack control formulas of each different standards or following proposed recommendations. One study[7-2] indicates that a maximum limit on steel stress of 36 ksi (250 MPa) would correspond to a maximum crack width of 0.01 inches (0.25 mm). This limit would also allow justification for assuming full continuity for negative moment analysis[7-3].

This chapter was mainly authored by Alex, Aríñez, Corres, El-Badry, Fernández-Ordóñez, García, Navarro, Petrangeli, Regúlez, Stucchi, Tadros, van der Zee, Waimberg, and Wheatley.

https://doi.org/10.35789/fib.BULL.0094.Ch07

8. Parametric study

8.1 Parametric analysis of effects of random variability time and materials properties

The restraining moment, due to volume change effects, is impacted by the random variability of construction schedules and material properties, especially creep and shrinkage values. The age of the beams when the bridge is made continuous determines how much beam creep and shrinkage have already occurred in the unrestrained state, and how much remains after continuity occurs. This is a condition over which a designer has little control.

To demonstrate the impact of the construction schedule, restraining moments were computed using beam ages of 7, 28, 42, 60, 90, and 120 days at the time of continuity. For the analysis, the basic data used for the example, such as beam type, spans, and concrete properties, are retained. Fig. 8-1 shows the results of the analysis. The figure includes the effect of temperature gradient and the elastic moment due to barrier loads. The figure shows that the restraining moment decreases rapidly in the early days and more slowly as the age approaches the 90 days recommended by AASHTO[8-1] (if detailed analysis is waived).

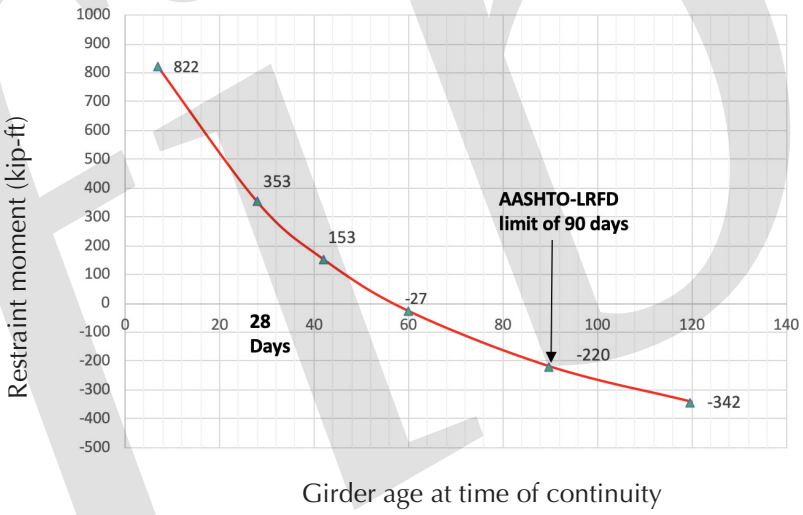

Fig. 8-1 Girder age at continuity versus restraint moment

The next parameter variability to study is the creep coefficient. This coefficient varies with environmental conditions, which are random and out of the control of the designer. Also, various codes have different prediction formulas. These formulas can result in variations of plus or minus 50%. The analysis revealed a near linear and proportionate relationship between the variation in creep and the magnitude of positive restraining moment (Fig. 8-2). A 50% change in creep results in almost 50% change in the restraining moment.

This chapter was mainly authored by Alex, Aríñez, Corres, El-Badry, Fernández-Ordóñez, García, Navarro, Petrangeli, Regúlez, Stucchi, Tadros, van der Zee, Waimberg, and Wheatley.
https://doi.org/10.35789/fib.BULL.0094.Ch08

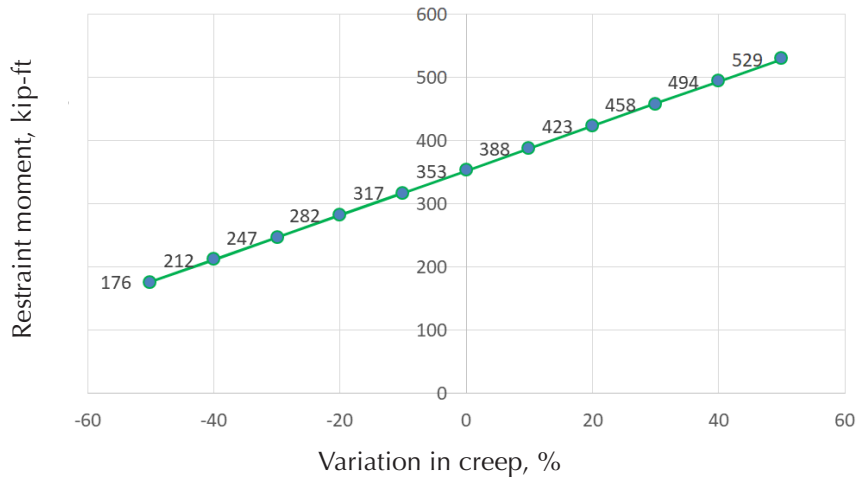

Fig. 8-2 Variability of creep causing effects versus magnitude of positive restraint moment. Note: 1 kip-ft = 1.356 kN-m

9. Examples

The magnitude of the results obtained in this example, positive restraint moment and reinforcement, is applicable to only one beam line. It should be multiplied by the number of beams for the total cross section.

9.1 Example 1

9.1.1 Description

The following example is a typical overpass bridge over interstate highway I-80 near Omaha, Nebraska, USA. The geometric properties, material properties, and environmental conditions are similar to what is generally assumed in that area of the United States.

Fig. 9-1 Example 1 bridge

9.1.2 Design specifications.

The bridge was designed using materials properties in accordance with the fourth edition of the AASHTO LRFD specifications with the 2016 Interim[9-1].

9.1.3 Bridge data

Geometry of the bridge	
Bridge width	15.20 m (50.00 ft)
Bridge length	54.90 m (180.00 ft)
Number of spans	2
Span length	27.40 m (90.00 ft)
Beam and slab geometry	
Beam depth	0.90 m (3.00 ft)
Beam gross section area	0.42 m2 (4.50 ft^2)

Example 1 was prepared by Tadros, Girgis, and Nickas.
Example 2 was prepared by Matute Rubio and Figueiredo.
Example 3 was prepared by De Chefdebien.

https://doi.org/10.35789/fib.BULL.0094.Ch09

Beam gross moment of inertia	0.46 m4 (53.10 ft^4)
Beam centroid to bottom fiber	0.41 m (1.30 ft)
Beam spacing	3.00 m (10.00 ft)
Slab thickness	0.20 m (0.70 ft)
Total depth of composite section	1.10 m (3.60 ft)

Dead loads

Beam self-weight	9.86 kN/m (0.68 kip/ft)
Deck self-weight	14.82 kN/m (0.97 kip/ft)
Barrier weight	2.92 kN/m (0.20 kip/ft)

The effects of future wearing surface and live loads are not included because these effects produce negative moments over the piers.

Prestressing

Number of prestressing strands	34
Effective area of strands	140.00 mm2 (0.22 in.^{2})
Prestressing stress (0.75F_{pu})	1'396.00 MPa (202.50 ksi)
Initial prestressing losses plus additional 5% for long-term prestressing losses	15%
Initial prestressing force (P)	5'649.00 kN (1'269.90 kip)

In this example, long-term prestressing losses have been considered, but they are counted as part of the initial prestressing force.

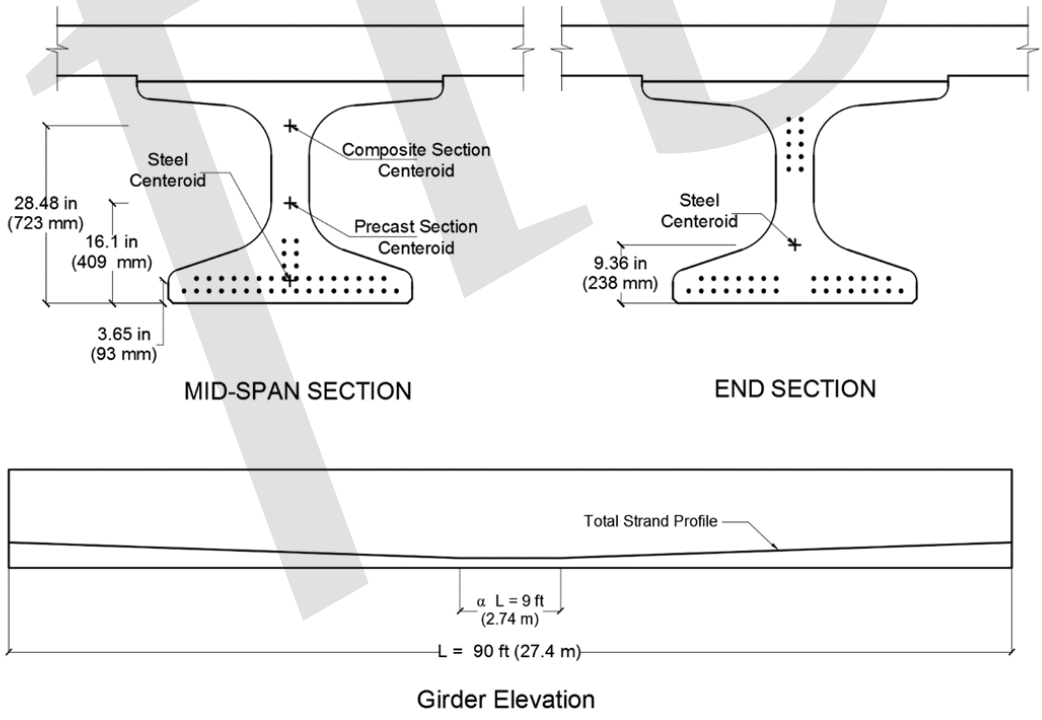

Fig. 9-2 Beam strand profile and cross sections. Note: L = span length; α_L = length of the beam with horizontal strands at its center

Eccentricity at beam ends in relation to beam centroid (e_e)	409.00 – 238.00 = 171.00 mm (6.70 in.)
Eccentricity at beam center in relation to beam centroid (e_c)	409.00-93.00 = 316.00 mm (12.45 in.)
Length of the beam with horizontal strands at its center (αL)	2.70 m (9.00 ft)

Time data

Prestressing strand release (t_0)	1 day
Diaphragm and deck construction (t_c)	28 days
End of beam life (t^∞)	27'000 days

This example assumes that the time at which the deck self-weight is applied on the beams is approximately equal to the time at which continuity is achieved.

Concrete strength

Beam at release	37.90 MPa (5.50 ksi)
Beam at 28 days	55.20 MPa (8.00 ksi)
Slab at 28 days	27.60 MPa (4.00 ksi)

Modulus of Elasticity

Beam initial (E_{ci})	30.40 GPa (4'406.00 ksi)
Beam at deck placement (E_c)	36.60 GPa (5'304.00 ksi)
Slab at 28 days (E_{cd})	25.10 GPa (3'644.00 ksi)

Creep coefficients

Beam	t_0 to t^∞ (φ_{bif})	1.53
	t_0 to t_c (φ_{bid})	0.63
	t_c to t^∞ (φ_{bdf})	1.03
Slab	t_c to t^∞ (φ_{sdf})	2.13

As a simplification, at infinite time, the aging factor adopted is equal to 0.70.

Shrinkage data

Relative humidity	70%
Differential shrinkage between girder and slab	274μ

9.1.4 Estimated bending moment over piers

In this simple example, there is only one pier diaphragm over which restraining moments due to continuity can develop. The center support is assumed not to allow for horizontal or vertical displacements. The abutment supports allow for horizontal but not vertical displacement. Simple formulas can be used for calculation of elastic, statically indeterminate bending moments over pier in this two-span simple case.

In this example, the elastic moment is estimated for the end of the beam at the face of diaphragm, not within the diaphragm, which is assumed to have a much larger cross section.

In this example, elastic moment due to prestressing was calculated using the composite section with its elastic properties for instantaneous (with no adjustment for creep effects, as explained in section 4.1). This is a conservative simplification.

9.1.4.1 Restraint moment due to prestress, beam weight, and deck weight

First, elastic analysis is performed, assuming that the load was introduced to a noncreeping continuous member.

M_o -928.00 m-kN (-685.00 ft-kip)

M_d -1'394.00 m-kN (-1'028.00 ft-kip)

M_p 4'792.00 m-kN (3'534.00 ft-kip)

For this specific example, the following analytic formula allows evaluation of the bending moments over the piers due to prestressing applied on the complete structure:

$$M = 0.75P\left[2e_e + (1+\alpha)(e_c - e_e)\right] = 4'792.00 \text{ m-kN } (3'533.00 \text{ ft-kip}) \quad (9\text{-}1)$$

In Eq. (9-1), the eccentricities relative to the composite beam/deck section should be used. Thus, e_e = 28.48 – 9.36 = 19.12 in. (486.00 mm), and e_c = 28.48 – 3.65 = 24.83 in. (631.00 mm).

Prestressing initially creates a negative moment at the end of the beam at the pier diaphragm. That moment is equal to the prestressing force multiplied by the eccentricity of the prestress force relative to the beam centroid: -5'649.00(0.41 – 0.24) = -967.30 m-kN (-713.30 ft-kip).

This initial prestress moment must be added to the other effects in estimating the net restraint moment.

Secondly, the time-dependent multipliers corresponding to the different loads are determined.

$$\delta_{B+P} = \frac{E_{B,tc}}{E_{B,t0}} \frac{\varphi_B(t_\infty, t_0) - \varphi_B(t_c, t_0)}{1 + \chi_B \cdot \varphi_B(t_\infty, t_c)} = 0.63 \quad (9\text{-}2)$$

$$\delta_{slab} = \frac{E_{B,tc}}{E_{B,tc}} \frac{\varphi_B(t_\infty, t_c) - \varphi_B(t_c, t_c)}{1 + \chi_B \cdot \varphi_B(t_\infty, t_c)} = \frac{\varphi_B(t_\infty, t_c)}{1 + \chi_B \cdot \varphi_B(t_\infty, t_c)} = 0.60 \quad (9\text{-}3)$$

Finally, the restraint moments are obtained:

$$M_{Beam\ weight} = \delta_{B+P} M_0 = -585.10 \text{ m-kN } (-431.70 \text{ ft-kip}) \quad (9\text{-}4)$$

$$M_{\text{Prestressing}} = \delta_{B+P} M_p + \text{initial moment} = 2'055.00 \text{ m-kN } (1'515.40 \text{ ft-kip}) \quad (9\text{-}5)$$

$$M_{\text{Slab weight}} = \delta_{\text{Slab}} \cdot M_d = -870.80 \text{ m-kN } (-642.20 \text{ ft-kip}) \quad (9\text{-}6)$$

9.1.4.2 Restraint moment due to superimposed dead load

M_{SIDL} -274.50 m-kN (-202.40 ft-kip)

9.1.4.3 Restraint moment due to slab shrinkage

Slab shrinkage strain (ε_s)	274μ
Age-adjusted force due to shrinkage $\varepsilon_s \cdot A_d \cdot E_{cd} / (1 + 0.7\psi_{ddf})$	1'713.60 kN (385.20 kip)
End moment due to shrinkage (M_{sh})	520.50 m-kN (383.80 ft-kip)

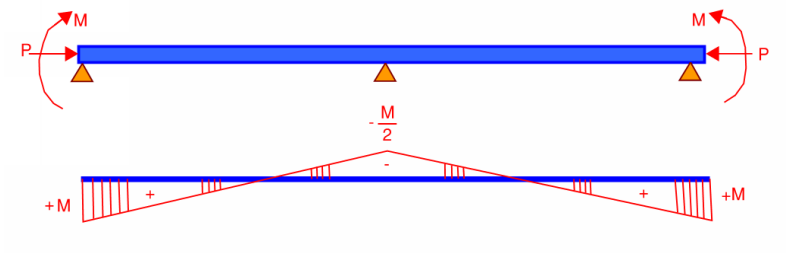

Fig. 9-3 Bending moment distribution for differential shrinkage. Note: M = moment; P = ?

Slab shrinkage restraint moment	-259.00 m-kN (-191.00 ft-kip)

9.1.4.4 Restraint moment due to thermal gradient

For this example, the cross-section geometry is simplified into layers of rectangular shapes. Furthermore, the temperature gradient is simplified into a series of constant rises in temperature (Fig. 9-4).

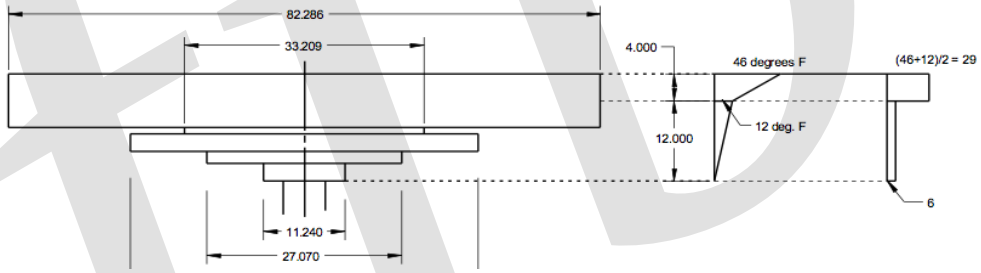

Fig. 9-4 Temperature gradient used for calculations. Note: All dimensions are in inches. 1 in. = 25.4 mm; °F = (°C × 1.8) + 32

Table 9-1 gives the calculations of the initial strains and restraining forces.

Table 9-1 Calculation of restraining moment due to temperature

Area no.	Width, in.	Depth, in.	Centroidal distance, in.	Temperature gradient	Restraining stress, ksi	Restraining force, kip	**Restraining moment, kip-ft**
1	82.286	4	13.96	29.00	0.925	304.36	4'247.8
2	82.286	4	9.96	6.00	0.191	62.97	627.0
3	33.209	1	7.46	6.00	0.191	6.35	47.4
4	48.430	2.5625	5.68	6.00	0.191	23.74	134.7
5	27.070	1.77	3.51	6.00	0.191	9.17	32.2
6	11.240	2.6875	1.28	6.00	0.191	5.78	7.4
						412.37	424.70
Total restraint moment							212.4

Note: 1 in. = 25.4 mm; 1 ksi = 6.895 MPa; 1 kip = 4.448 kN; 1 kip-ft = 1.356 kN-m.

Restraining moment due to thermal load	288.00 m-kN (212.40 ft-kip)

9.1.4.5 Net restraint moment due to total effects

Table 9-2 Calculation of total restraint moment

Effect	Elastic moment on complete structure, m-kN (ft-kip)	Time-dependent multiplier	Restrain moment over pier, m-kN (ft-kip)
Beam self-weight	-928.20 (-684.50)	0.63	-585.40 (-431.70)
Prestressing	4'791.90 (3'533.60)	0.63	2'055.00 (1515.40)
Slab self-weight	-1'394.20 (-1'028.10)	0.60	-833.80 (-614.80)
Superimposed dead load	-274.50 (-202.40)	1.00	-274.50 (-202.40)
Shrinkage	-259.00 (-191.00)	Not applicable	-259.00 (-191.00)
Temperature	288.00 (121.40)	1.00	288.00 (212.40)
Total restraint moment			390.30 (287.90)

9.1.5 Determination of the reinforcement in the bottom flange of the continuity diaphragm

Due to cracking in the beam adjacent to the pier diaphragm, moment redistribution is expected to occur. For this reason, it is conservative to assume a 10% reduction factor in the moment calculated in Table 9-2, which was based on an uncracked member.

A simplified method is used in which a maximum stress is assumed at the steel reinforcement to control cracking.

The stress limit is assumed to be 250.00 MPa (36.00 ksi).

The minimum corresponding area of steel is calculated with Eq. (9-7):

$$A_{s,req} = \frac{0.9M_d}{z \cdot \sigma_{s,\lim}} = \frac{390.3 \cdot 0.9}{0.903 \cdot 248'000} = 15.70 \text{ cm}^2 \left(2.43 \text{ in.}^2\right) \quad (9\text{-}7)$$

where z is the lever arm between tension and compression, assuming $0.80h$ = 903.00 mm (35.55 in.)

The corresponding number of 0.6 in. (15.20 mm) diameter strands to be extended and bent into the diaphragm = 15.7/1.4 = 11.20. Use 12 bent strands. Extend the strands 6 in. (150.00 mm) horizontally and 18 in. (450.00 mm) vertically into the diaphragm to allow for adequate bond to the cast-in-place concrete.

9.1.6 Detail adopted over the pier

Fig. 9-5 Bridge under construction near Des Moines, Iowa, US. Note bent strands

9.2 Example 2

9.2.1 Description

The viaduct has two parallel bridges, each with a continuous precast concrete structure. Each superstructure has four I-girders with a total depth of 2.00 m (6.60 ft) and a 25.00 cm (10 in.) cast-in-place slab. The girder spacing is 3.50 m (11.50 ft).

Fig. 9-6 View of the Example 2 bridge

The superstructure has 10 continuous spans of 35.00 m (115 ft), and a total width of 13.10 m (43.00 ft). Superstructure continuity is established only for superimposed dead loads (SIDL) and live loads (LL), using continuity end diaphragms.

9.2.2 Design code

RSA – Regulamento de Segurança e Ações (Portuguese standard)

9.2.3 Bridge data

Geometry of the bridge	
Bridge width	13.10 m (43.00 ft)
Bridge length	350.00 m (1'148.30 ft)
Number of spans	10
Span length	35.00 m (114.80 ft)

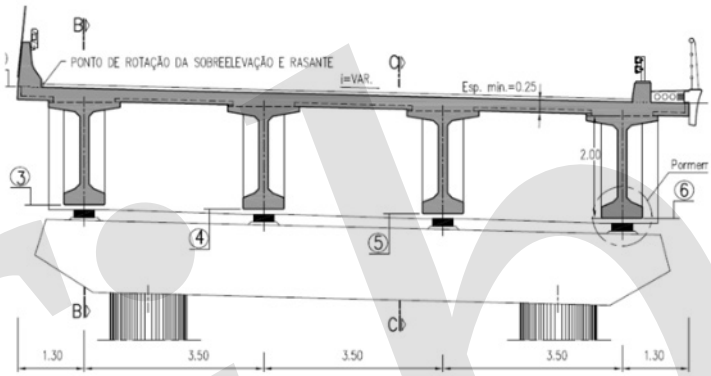

Fig. 9-7 Bridge cross section over piers

Beam and slab geometry	
Beam depth	2.00 m (6.60 ft)
Beam gross section area	0.73 m^2 (7.90 ft^2)
Beam gross moment of inertia	0.41 m^4 (48.00 ft^4)
Beam centroid to bottom fiber	1.03 m (3.40 ft)
Beam spacing	3.50 m (11.50 ft
Slab thickness	0.25 m (0.80 ft)
Total depth of composite section	2.25 m (7.40 ft)
Dead loads	
Beam self-weight	18.34 kN/m (1.26 kip/ft)
Deck self-weight	21.88 kN/m (1.50 kip/ft)
Barrier and sidewalk weight	21.00 kN/m (1.44 kip/ft)
Wearing surface (including repaving)	34.50 kN/m (2.37 kip/ft)
Live loads	
Uniform load	4.00 kN/m2 (0.58 psi)
Transverse line load	50.00 kN/m (3.57 kip/ft)

Truck load, three axles	200.00 kN/axle (44.96 kip/axle)
Sidewalk	3.00 kN/m^2 (0.44 psi)
Prestressing	
Number of prestressing strands	32
Effective area of strands	140.00 mm^2 (0.22 in.^{2})
Prestressing stress (0.75F_{pu})	1'396.00 MPa (202.50 ksi)
Initial prestressing losses	15%
Initial prestressing force (P)	5'312.00 kN (1'194.30 kip)
Long-term prestressing losses	15%

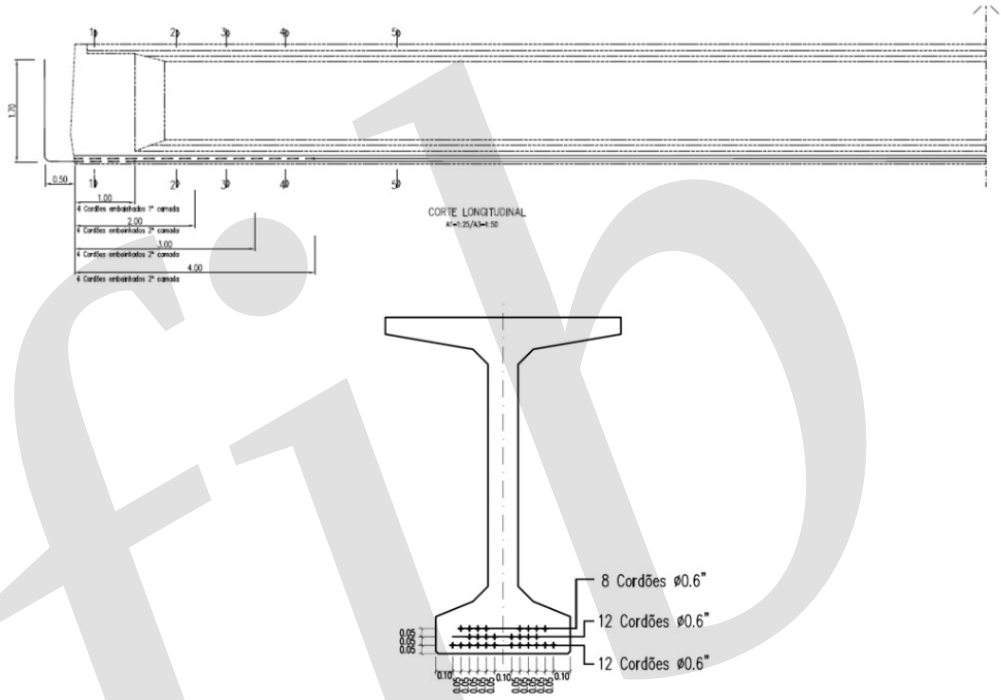

Fig. 9-8 Beam strand profile

Concrete strength	
Beam at release (f_{ck})	40.00 MPa (5.80 ksi)
Beam at 28 days (f_{ck})	40.00 MPa (5.80 ksi)
Slab at 28 days (f_{ck})	35.00 MPa (5.08 ksi)
Steel strength	
Reinforcement (f_y)	500.00 MPa (72.60 ksi)
Prestressing (f_{puk})	1'860.00 MPa (269.90 ksi)
Shrinkage data	
Relative humidity	70%
Differential shrinkage between girder and slab	150μ

9.2.4 Estimated bending moment over piers

Assuming all continuity details are equal, the bending moments over the piers are estimated over the second support, because the maximum bending moments occur in this section.

In this example, as often happens in engineering design, the time in which continuity takes place is unknown. Consequently, for the estimation of restraint moments due to loads applied before continuity, we assume two values of δ.

The first value (0.50) leads to a lower level of redistribution, and can occur if continuity is established a long time after the girders have been cast. The second value (0.80) corresponds to the opposite situation, where continuity is established at a young age.

In this example, we have developed the calculations corresponding to the value of $\delta = 0.80$ because it produces the maximum positive moments over the piers.

As a simplification, at infinite time, the aging factor is equal to 0.80.

Additionally, the moduli of elasticity used in the equivalent moduli of elasticity to calculate the centroid of the complete section correspond to the 28-day modulus for the beam and the deck.

9.2.4.1 Restraint moment due to prestress, beam weight, and deck weight

First, elastic analysis is carried out, assuming that the load was introduced to a noncreeping continuous member.

M_0 -2'373.30 m-kN (-1'750.60 ft-kip)
M_d -2'831.30 m-kN (-2'088.00 ft-kip)
M_p 8'715.80 m-kN (6'427.60 ft-kip)

Fig. 9-9 Bending moment distribution due to prestressing

M_{pl} -1'308.40 m-kN (-964.10 ft-kip)

Second, the time-dependent multipliers corresponding to the different loads are determined.

$$\delta_{B+P} = \frac{E_{B,tc}}{E_{B,t0}} \frac{\varphi_B(t_\infty,t_0) - \varphi_B(t_c,t_0)}{1+\chi_B \cdot \varphi_B(t_\infty,t_c)} \cong 0.80 \tag{9-8}$$

$$\delta_{Slab} = \frac{E_{B,tc}}{E_{B,tc}} \frac{\varphi_B(t_\infty,t_c) - \varphi_B(t_c,t_c)}{1+\chi_B \cdot \varphi_B(t_\infty,t_c)} = \frac{\varphi_B(t_\infty,t_c)}{1+\chi_B \cdot \varphi_B(t_\infty,t_c)} \cong 0.80 \tag{9-9}$$

$$\delta_{Losses} = \frac{E_{B,tc}}{E_{B,t0}} \frac{\chi_B\left[\varphi_B(t_\infty,t_0) - \varphi_B(t_c,t_0)\right]}{1+\chi_B \cdot \varphi_B(t_\infty,t_c)} \cong 0.80\chi_B = 0.64 \tag{9-10}$$

Finally, the restraint moments are obtained:

$$M_{\text{Beam weight}} = \delta_{B+P} \cdot M_0 = -1'899.00 \text{ m-kN } (-1400.00 \text{ ft-kip}) \quad (9\text{-}11)$$

$$M_{\text{Prestressing}} = \delta_{B+P} \cdot M_p = 6'973.00 \text{ m-kN } (5'142.00 \text{ ft-kip}) \quad (9\text{-}12)$$

$$M_{\text{Slab weight}} = \delta_{\text{Slab}} \cdot M_d = -2'265.00 \text{ m-kN} (-1'670.00 \text{ ft-kip}) \quad (9\text{-}13)$$

9.2.4.1.1 Restraint moment due to superimposed dead load and live load:

These loads act directly on the final structural system and consequently there is no creep restraint moment due to these loads.

M_{SIDL} -2'075.00 m-kN (-1'530.00 ft-kip)

M_{LL} 310.00 m-kN (229.00 ft-kip)
(maximum positive bending moment considered)

9.2.4.1.2 Restraint moment due to slab shrinkage

For this case, no differential shrinkage between deck and beam was considered at the sections over piers.

Slab shrinkage strain (ε_s)	150m
Age-adjusted force due to shrinkage $\varepsilon_s A_d E_{cd}/(1+0.7\psi_{ddf})$	1'195.00 kN (269.00 kip)
End moment caused due to shrinkage (M_{sh})	725.00 m-kN (535.00 ft-kip)

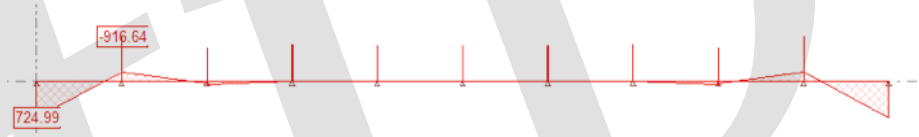

Fig. 9-10 Bending moment distribution due to shrinkage

Deck shrinkage restraint moment -916.00 m-kN (-676.00 ft-kip)

9.2.4.1.3 Restraint moment due to thermal gradient

The effects of thermal load are calculated similarly to the deck shrinkage but using short-term constants for the complete section.

Temperature gradients (TG):	
Positive gradient (TG +)	+10.00°C (18°F)
Negative gradient (TG -)	-5.00°C (-9°F)
Restraint moment due to thermal load	1'675.00 m-kN (1'235.00 ft-kip)

9.2.4.2 Net restraint moment due to total effects

Table 9-3 Calculation of total restraint moment

Effect	**Elastic moment on complete structure m-kN (ft-kip)**	**Time-dependent multiplier δ**	**Restraint moment over pier m-kN (ft-kip)**
Beam self-weight	-2'373.30 (-1'750.60)	0.80	-1'899.00 (-1'400.40)
Prestressing	8'715.80 (6'427.60)	0.80	6'972.60 (5'142.10)
Slab self-weight	-2'831.30 (-2.88.00)	0.80	-2'265.00 (-1'670.40)
Long-term prestressing losses	-1'308.40 (-964.10)	0.64	-836.70 (-617.00)
Superimposed dead load	-2'075.00 (-1'530.30)	1.00	-2'075.00 (-1'530.30)
Live load	310.00 (228.60)	1.00	310.00 (228.60)
Shrinkage	-916.00 (-675.50)	Not applicable	-916.00 (-675.50)
Temperature	1'675.00 (1'235.20)	1.00	1'675.00 (1'235.20)
Total restraint moment			**965.90 (712.30)**

9.2.5 Determination of the reinforcement in the bottom flange of the continuity diaphragm

To control cracking, the steel stress is limited to a maximum value of 248 MPa (36 ksi).

Therefore, the minimum corresponding area of steel would be:

$$A_{s,req} = \frac{M_d}{z \cdot \sigma_{s,\lim}} = \frac{965.9}{1.823 \cdot 248'000} = 22 \text{ cm}^2 \ \left(3.87 \text{ in.}^2\right) \qquad (9\text{-}15)$$

where z is the lever arm, assuming $0.81h$ = 1'823.00 mm (71.80 in.)

9.2.6 Detail adopted over the pier

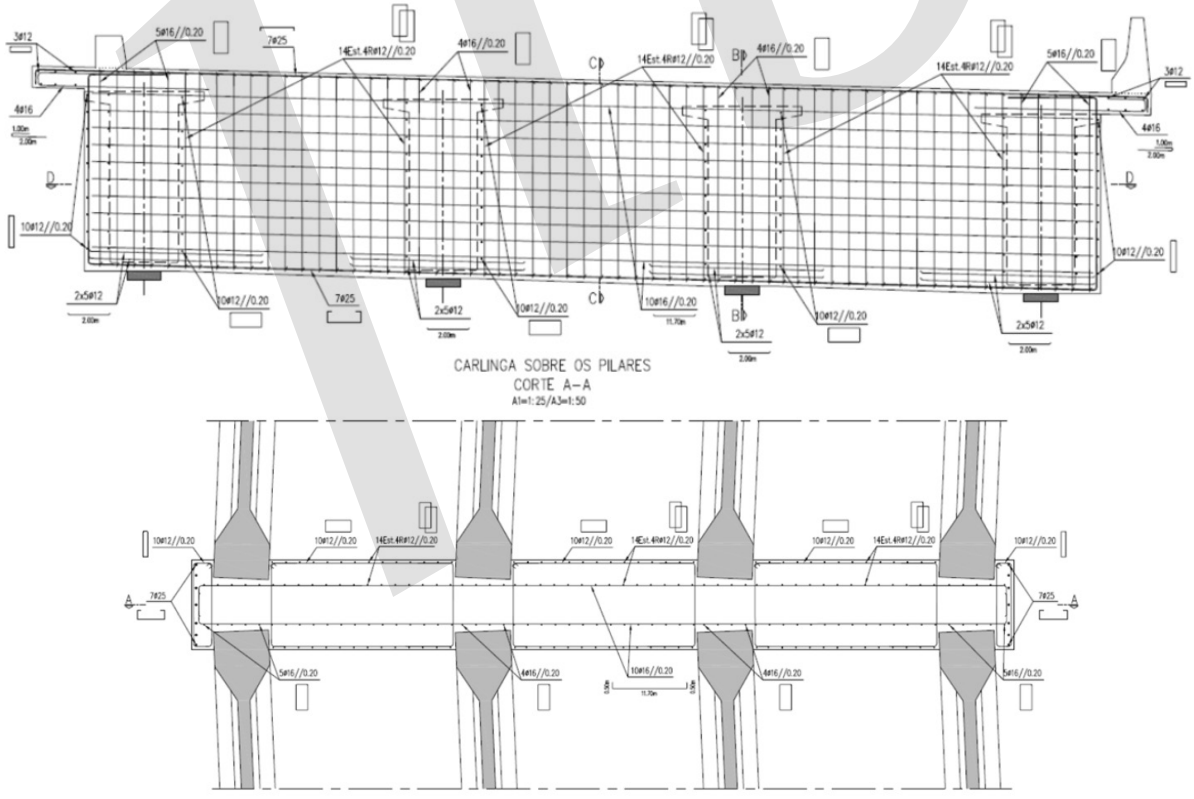

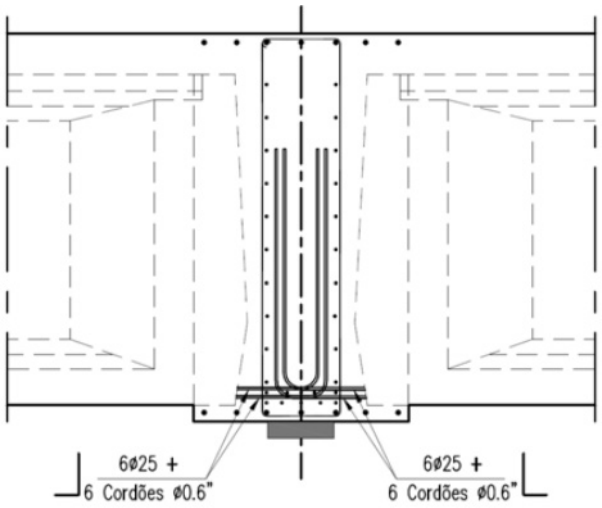

Fig. 9-11 Reinforcement detail over piers

9.3 Example 3

9.3.1 Description

The bridge has seven I-girders with a total depth of 0.95 m (3.1 ft) and a 20.00 cm (7.9 in.) cast-in-place slab. The girder spacing is 1.25 m (4.10 ft).

Fig. 9-12 Example 3 bridge

The deck has two continuous spans of 23.00 m (90.00 ft). The deck width is 8.50 m (27.9 ft). Deck continuity is established only for SIDL and LL loads, using continuity end diaphragms.

9.3.2 Design code

The bridge was designed in accordance with EN 1992.

9.3.2 Bridge data

Geometry of the bridge	
Bridge width	8.50 m (27.9 ft)
Bridge length	46.00 m (150.88 ft)
Number of spans	2
Span length	23.00 m (75.44 ft)

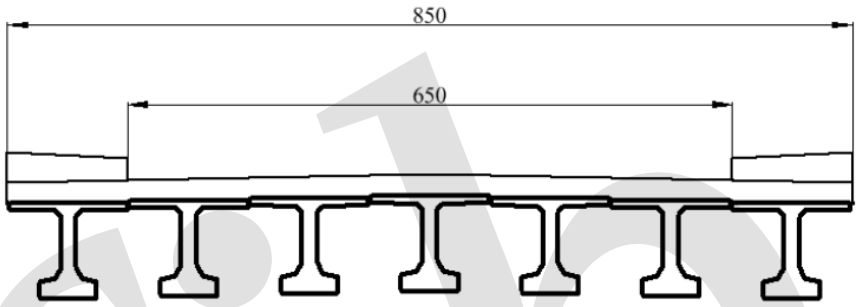

Fig. 9-13 Bridge cross section. Note: All dimensions are in centimeters. 1 cm = 0.39 in

Beam and slab geometry	
Beam depth	0.95 m (3.11 ft)
Beam gross section area	0.30 m2 (3.28 ft^2)
Beam gross moment of inertia	0.04 m4 (4.40 ft^4)
Beam centroid to bottom fiber	0.48 m (1.59 ft)
Beam spacing	1.25 m (4.10 ft)
Slab thickness	0.20 m (0.70 ft)
Total depth of composite section	1.15 m (3.80 ft)
Dead loads	
Beam self-weight	7.63 kN/m (0.52 kip/ft)
Deck weight	6.25 kN/m (0.43 kip/ft)
Barrier weight	2.92 kN/m (0.20 kip/ft)
Prestressing	
Number of prestressing strands	14
Effective area of strands	150.00 mm2 (0.25 $in.^2$)
Prestressing stress (095F_{py})	1'560 MPa (226.5 ksi)
Initial prestressing losses	15%
Initial prestressing force (P)	2'786 kN (1'581.90 kip)
Long-term prestressing losses	15%

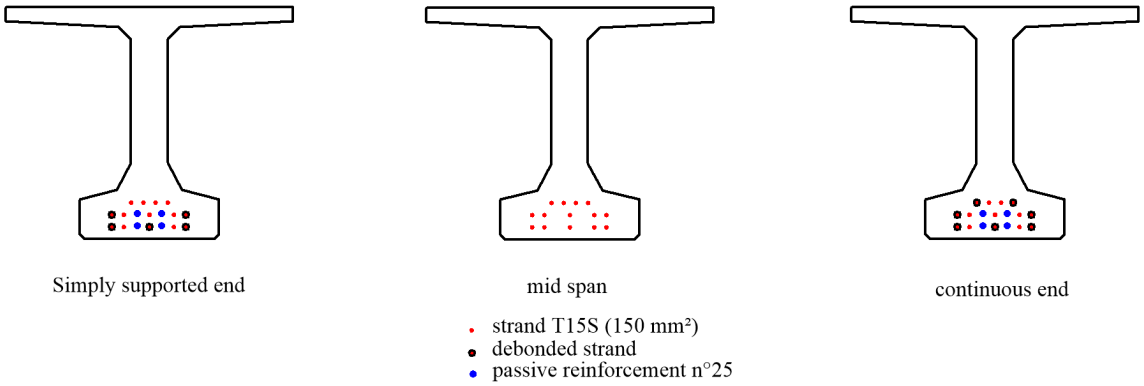

Fig. 9-14 Prestressing scheme

Time data	
Prestressing strand release (t_0)	1 day
Diaphragm and deck construction (t_c)	40 days
End of beam life (t^∞)	35'000 days
Concrete strength	
Beam at release (f_{ck})	37.90 MPa (5.50 ksi)
Beam at 28 days (f_{ck})	60.00 MPa (8.70 ksi)
Slab at 28 days (f_{ck})	35.00 MPa (5.08 ksi)
Modulus of elasticity	
Beam initial (E_{ci})	39.10 GPa (5.67 ksi)
Beam at deck placement (E_c)	39.10 GPa (5.67 ksi)
Slab at 28 days (E_{cd})	34.10 GPa (4.94 ksi)

The moduli of elasticity of beam and deck are considered to remain constant through time in this example.

Creep coefficients		
Beam	t_0 to t^∞ φ_{bif}	2.20
	t_0 to t_c φ_{bid}	1.05
	t_c to t^∞ φ_{bdf}	1.11
Slab	t_c to t^∞ φ_{sdf}	3.23

As a simplification, at infinite time, the aging factor adopted is equal to 0.80.

Relative humidity	70%

9.3.4 Estimated bending moment over piers

In this example, there is only one pier section over which restraining moments can develop due to continuity.

The effect of differential shrinkage between deck and beam and the effect of thermal gradient are not considered in this example.

9.3.4.1 Restraint moment due to prestress, beam weight and deck weight

First, elastic analysis is performed, assuming that the load was introduced to a noncreeping continuous member.

M_0 -504.50 m-kN (-372.10 ft-kip)

M_d -413.30 m-kN (-304.80 ft-kip)

M_p 1'817.00 m-kN (1'340.15 ft-kip)

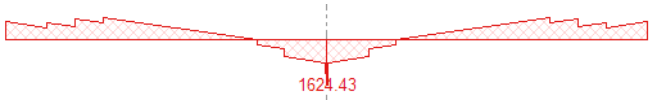

Fig. 9-15 Bending moment distribution due to prestressing. All dimensions are in m-kN

M_{pl} -273.00 m-kN (-180.10 ft-kip)

Second, the time-dependent multipliers corresponding to the different loads are determined.

$$\delta_{B+P} = \frac{E_{B,tc}}{E_{B,t0}} \frac{\varphi_B(t_\infty,t_0) - \varphi_B(t_c,t_0)}{1+\chi_B \cdot \varphi_B(t_\infty,t_c)} = 0.61 \tag{9-16}$$

$$\delta_{Slab} = \frac{E_{B,tc}}{E_{B,tc}} \frac{\varphi_B(t_\infty,t_c) - \varphi_B(t_c,t_c)}{1+\chi_B \cdot \varphi_B(t_\infty,t_c)} = \frac{\varphi_B(t_\infty,t_c)}{1+\chi_B \cdot \varphi_B(t_\infty,t_c)} = 0.59 \tag{9-17}$$

$$\delta_{Losses} = \frac{E_{B,tc}}{E_{B,t0}} \frac{\chi_B\left[\varphi_B(t_\infty,t_0) - \varphi_B(t_c,t_0)\right]}{1+\chi_B \cdot \varphi_B(t_\infty,t_c)} = 0.49 \tag{9-18}$$

Finally, the restraint moments are obtained:

$$M_{\text{Beam weight}} = \delta_{B+P} \cdot M_0 = -307.70 \text{ m-kN } (-2'226.95 \text{ ft-kip}) \tag{9-19}$$

$$M_{\text{Prestressing}} = \delta_{B+P} \cdot M_p = 1'108.50 \text{ m-kN } (817.59 \text{ ft-kip}) \tag{9-20}$$

$$M_{\text{Deck weight}} = \delta_{\text{Slab}} \cdot M_d = -243.80 \text{ m-kN } (-179.82 \text{ ft-kip}) \tag{9-21}$$

$$M_{Losses} = \delta_{Losses} \cdot M_{pl} = -134.00 \text{ m-kN } (-98.83 \text{ ft-kip}) \tag{9-22}$$

9.3.4.2 Restraint moment due to superimposed dead load

M_{SIDL} -248.00 m-kN (-182.90 ft-kip)

9.3.4.3 Net restraint moment due to total effects

Table 9-4 Calculation of total restraint moment

Effect	Elastic moment on complete structure m-kN (ft-kip)	Time-dependent multiplier δ	Restraint moment over pier m-kN (ft-kip)
Beam self-weight	-504.50 (-372.10)	0.61	-309.30 (-228.00)
Prestressing	1'817.00 (1'340.15)	0.61	1'108.50 (817.59)
Slab self-weight	-413.30 (-304.80)	0.59	-242.70 (-179.00)
Long-term prestressing losses	-273.00 (-201.35)	0.49	-134.00 (-98.83)
Superimposed dead load	-248.00 (-182.90)	1.00	-248.00 (-182.90)
Total restraint moment			**175.20 (129.22)**

9.3.5 Determination of the reinforcement in the bottom flange of the continuity diaphragm

A simplified method is used in which a maximum stress is assumed at the steel reinforcement to control cracking.

The stress limit is assumed to be 248 MPa (36 ksi).

The minimum corresponding area of steel:

$$A_{s,req} = \frac{M_d}{z \cdot \sigma_{s,\lim}} = \frac{175}{0.9315 \cdot 248'000} = 7.58 \text{ cm}^2 \left(1.17 \text{ in.}^2\right) \quad (9\text{-}23)$$

where z is the lever arm between tension and compression, assuming $0.81h$ = 931.50 mm (36.70 in.)

This steel section should be added to the steel section necessary to control the crack opening under thermal gradient (and accidental settlement). In the present case the moment due to thermal restraint (frequent combination value) is equal to 225.00 m-kN.

9.3.6 Detail adopted over the pier

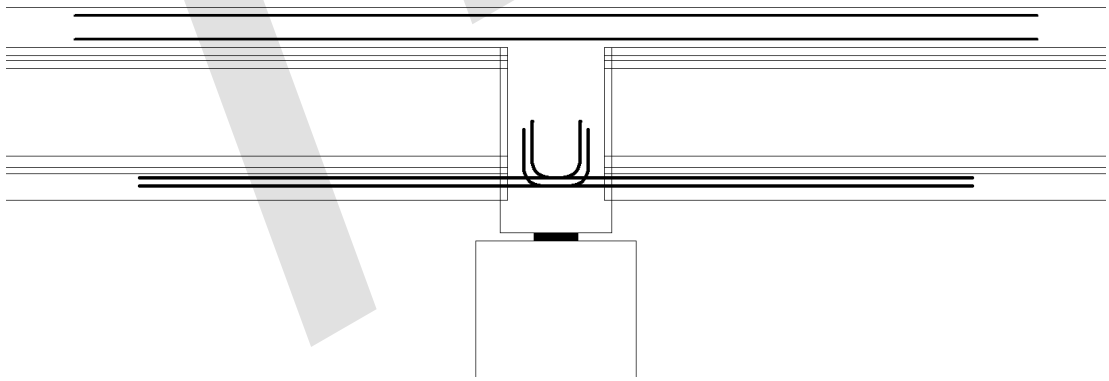

Fig. 9-16 Reinforcement detail over pier

10. References

The references below are directly cited in the document. The bibliography in the next section contains relevant resources that are intended to help the readers get a deeper understanding of the technical issues covered in this document.

Chapter 4

[4-1] Mattock, A.H., and Kaar, P.H., "Continuous Precast-Prestressed Concrete Bridges. Development Department Bulletin D43," *Portland Cement Association, Research and Development Laboratories*, Vol.3, No.2. Stokie, Illinois, (1961).

[4-2] Freyermuth, C.L., "Design of Continuous Highway bridges with Precast, Prestressed Concrete Girders," *Journal of the Prestressed Concrete Institute*, Vol.14, No.2, April 1969; pp.14-39. Also reprinted as PCA *Engineering Bulletin EB014.01E*, August (1969).

[4-3] Bazant, Z.P." Theory of Creep and Shrinkage in Concrete Structures: A précis of recent developments." *Mechanics today*. American Academy of Mechanics, Vol.2. Pergamon, New York. (1975).

[4-4] Tadros, M. K., Ghali, A., and Dilger,W. H., "Time-Dependent Analysis of Composite Frames," *Journal of the Structural Division*, ASCE, V. 103, No.ST4, Proceedings Paper 12893, April1977, pp. 871-884, (1977).

[4-5] Tadros, M.K., Ghali, A. and Meyer, A.W., "Prestress Loss and Deflection of Precast Members," *PCI Journal*, Vol.30, No.1, Chicago, IL January- February 1985 pp. 114-141, (1985).

[4-6] Dilger, W. H., "Creep Analysis Using Creep-Transformed Section Properties." *J. Prestressed Concrete Institute*, Vol. 27, No.1 (1982) pp. 98-117, (1982).

[4-7] Oesterle, R.G., Glikin, J.D., and Larson, S.C. NCHRP report 322: Design of Precast Prestressed Bridge Girders Made Continuous. Transportation Research Board, National Research Council; Washington, DC; November, (1989).

[4-8] Pérez Caldentey (1996), "Comportamiento en servicio del hormigón estructural. Estudio teórico y experimental". Tesis Doctoral. E.T.S.I. Caminos, Canales y Puertos. Universidad Politécnica de Madrid, (1996).

[4-9] Ghali, A., R. Favre, and M. Elbadry, *Concrete Structures: Stresses and Deformations - Analysis and Design for Serviceability*, Fourth Edition. Spon Press, (2012).

[4-10] Miller, R.A., Castrodale, R.W., Mirmiran, A., and Hastak, M. "Connection of simple Span Precast Concrete Girders for Continuity". National Cooperative Highway Research Program, Report 519, (2004).

[4-11] Oesterle, R.G., Glikin, J.D., and Larson, S.C. NCHRP report 322: "Design of Precast Prestressed Bridge Girders Made Continuous". Transportation Research Board, National Research Council; Washington, DC; November, (1989).

This chapter was mainly authored by Aríñez, Corres, Navarro, Regúlez, Tadros.

https://doi.org/10.35789/fib.BULL.0094.Ch10

Chapter 5

[5-1] Eurocode 2 (EN 1992-2), Design of Concrete Structures. Part 2. Concrete Bridges. Design and Detailing Rules, CEN, (2005).

[5-2] Ghali, A., R. Favre, and M. Elbadry, *Concrete Structures: Stresses and Deformations - Analysis and Design for Serviceability*, Fourth Edition. Spon Press, (2012).

[5-3] Trost, H. Creep, "Relaxation and Shrinkage of Structural Concrete". IABSE Colloquium *Structural Concrete*. Stuttgart, (1991).

[5-4] Trost, H. "Implications of the Superposition Principle in Creep and Relaxation Problems for Concrete and Prestressed Concrete", *Beton und Stahl-Beton Bau* No. 10, , pp. 230-238, 261-269, (1967).

[5-5] Bazant, Z.P." Theory of Creep and Shrinkage in Concrete Structures: A précis of recent developments." *Mechanics today*. American Academy of Mechanics, Vol.2. Pergamon, New York. (1975).

[5-6] AASHTO (American Association of State Highway and Transportation Officials), *AASHTO LRFD Bridge Design Specifications*, 7th Edition. Washington, DC., with the 2016 Interim Revisions, (2016).

[5-7] Model Code 2010. Bulletin d'Information No 65/66. *fib*, (2010).

[5-8] Müller, H. S., F. Acosta, *Time Dependent Effects of Structural Concrete: Basics for Constitutive Modelling towards the Next Generation of Eurocode 2*, (2014).

Chapter 6

[6-1] Eurocode 2 (EN 1992-2), Design of Concrete Structures. Part 2. Concrete Bridges. Design and Detailing Rules, CEN, (2005).

[6-2] PCI. 2014. *Bridge Design Manual*, Third Edition, Second Release, (MNL-133-14). Precast/Prestressed Concrete Institute, Chicago, IL. 1620 pp., (2011).

[6-3] EHE-08, Instrucción de Hormigón Estructural. Ministerio de Fomento, (2008).

[6-4] Ghali, A., R. Favre, and M. Elbadry, *Concrete Structures: Stresses and Deformations - Analysis and Design for Serviceability*, Fourth Edition. Spon Press, (2012).

[6-5] Model Code 1990. Bulletin d'Information No 213/214. May 1993. CEB-FIP, (1993).

[6-6] AASHTO (American Association of State Highway and Transportation Officials), *AASHTO LRFD Bridge Design Specifications*, 7th Edition. Washington, DC., with the 2016 Interim Revisions, (2016).

Chapter 7

[7-1] AASHTO (American Association of State Highway and Transportation Officials), *AASHTO LRFD Bridge Design Specifications*, 7th Edition. Washington, DC., with the 2016 Interim Revisions, (2016).

[7-2] Frosch, R.J., "Another look at Cracking and Crack control in Reinforced Concrete," *ACI Structural Journal*, May-June (1999).

[7-3] Miller, R.A., Castrodale, R.W., Mirmiran, A., and Hastak, M. "Connection of simple Span Precast Concrete Girders for Continuity". National Cooperative Highway Research Program, Report 519, (2004).

Chapter 8

[8-1] AASHTO (American Association of State Highway and Transportation Officials), *AASHTO LRFD Bridge Design Specifications*, 7th Edition. Washington, DC., with the 2016 Interim Revisions, (2016).

Chapter 9

[9-1] AASHTO (American Association of State Highway and Transportation Officials), *AASHTO LRFD Bridge Design Specifications*, 7th Edition. Washington, DC., with the 2016 Interim Revisions, (2016).

11. Bibliography

The references in the preceding section are directly cited in the document. The bibliography in this section contains relevant resources that are intended to help the readers get a deeper understanding of the technical issues covered in this document.

Aluthjage Don Chandrathilaka Jayanandana "Continuity Development between Precast Beams using Prestressed Slabs, and its Effect on Flexure and Shear" PhD Thesis. University of Leeds (1989).

CEB, *Structural Effects of Time-Dependent Behaviour of Concrete*. Bulletin d'Information N°142, (1984).

Chiorino, M. A., Giuseppe Lacidogna, "Approximate Values of the Aging Coefficient for the Age-Adjusted Effective Modulus Methods in Linear Analysis of Concrete Structures", *CEB Model 1990 for Creep*, Atti del Dipartimento di Ingegneria Strutturale, Politecnico di Torino, (1991).

Dwairi, Hazim M., Matthew C. Wagner, Mervyn J. Kowalsky, and Paul Zia "Behavior of Instrumented Prestressed High Performance Concrete Bridge Girders" *Construction and Building Materials* 24, (2010).

J.F.Millanes "Un método general de cálculo para el seguimiento de la historia tensodeformacional en tableros de puentes construidos de forma evolutiva" *Hormigón y Acero* Nº 156.

Kumar, Venkatesh, R. Kodur and T. I. Campbell "Evaluation of Moment Redistribution in a Two-Span Continuous Prestressed Concrete Beam" *ACI Structural Journal* 93-S69, (1993).

Lin, T.Y. and Keith Thornton. 1972. "Secondary Moment and Moment Redistribution in Continuous Prestressed Concrete Beams" *PCI Journal*, Precast/Prestressed Concrete Institute, Chicago, IL. V. 17, No.1 (January-February), pp. 8-20, (1972).

Lopes, Sergio M. R., J. Harrop and A. E. Gamble. 1997. "Study of Moment Redistribution In Prestressed Concrete Beams" *Journal of Structural Engineering*, American Society of Civil Engineers, Reston, VA. V. 123, Issue 5. (May), (1997)

Snezana R. Mašovic , Saša R. Stošic, Nenad P. Pecic, "Research of long-term behaviour of non-prestressed precast concrete beams made continuous" *Engineering Structures* 70, (2014).

Sousa, Carlos, Marco Fonseca, Rui Calçada, and Afonso Serra Neves "New Methodology for Calculation of Required Prestressing Levels in Continuous Precast Bridge Decks" *ASCE Journal of Bridge Engineering* November (2013).

Sousa, Carlos, Helder Sousa, Afonso Serra Neves, and, Joaquim Figueiras. 2012. "Numerical Evaluation of the Long-Term Behavior of Precast Continuous Bridge Decks" *ASCE Journal of Bridge Engineering*, (January/February), 26pp., (2012).

Trost, H. "Spannungs,-Dehnungs-Gesetz eines viskoestastischen Festkörpers wie Beton und Folgerungen für Stabwerke aus Stahl-Beton und Spannbeton". *Beton* 16, No. 6, (1966).

This chapter was mainly authored by Aríñez, Corres, Navarro, Regúlez, Tadros.

https://doi.org/10.35789/fib.BULL.0094.Ch11

The *fib* (International Federation for Structural Concrete - Fédération internationale du béton) is grateful for the invaluable support of the following national member groups and sponsoring members, which contributes to the publication of *fib* technical bulletins, the *Structural Concrete* journal and *fib*-news.

National member groups

UNNOBA - Universidad Nacional del Nor Oeste de la Provincia de Buenos Aires, Argentina
CIA - Concrete Institute of Australia
ÖBV - Österreichische Bautechnik Vereinigung, Austria
GBB-BBG - Groupement Belge du Béton, Belgium
ABCIC - Associação Brasileira da Construção Industrializada de Concreto, Brazil
ABECE - Associação Brasileira de Engenharia e Consultoria Estrutural, Brazil
IBRACON - Instituto Brasileiro do Concreto, Brazil
CPCI (Canadian Precast Prestressed Concrete Institute)
Université Laval, Canada
CCES - China Civil Engineering Society
Cyprus University of Technology
Cyprus Association of Civil Engineers
Česká Betonářská Společnost, Czech Republic
DBF - Dansk Betonforening, Denmark
SB - Suomen Betoniyhdistys, Finland
AFGC - Association Française de Génie Civil, France
DAfStb - Deutscher Ausschuss für Stahlbeton, Germany
Technical Chamber of Greece
University of Patras, Department of Civil Engineering, Greece
Hungarian Group of the *fib*
The Institution of Engineers, India
fib-Indonesia
University of Amirkabir, Iran
IACIE - Israeli Association of Construction and Infrastructure Engineers
AICAP - Associazione Italiana Calcestruzzo, Armato e Precompresso, Italy
CTE - Collegio dei tecnici della industrializzazione edilizia, Italy
ITC - CNR, Istituto per le Tecnologie della Costruzione, Italy
ReLUIS, Italy
JCI - Japan Concrete Institute
JPCI - Japan Prestressed Concrete Institute
Administration des Ponts et Chaussées, Luxembourg
fib Netherlands
NZCS - New Zealand Concrete Society
NB - Norsk Betongforening / Norwegian Concrete Association
Polish Academy of Sciences, Committee for Civil Engineering, Poland
GPBE - Grupo Português de Betão Estrutural, Portugal
Polytechnic University of Timisoara, Romania
Technical University of Civil Engineering, Romania
University of Transylvania Brasov, Faculty of Civil Engineering, Romania
Association for Structural Concrete, Russia
SNK *fib*, Slovakia
Slovenian Society of Structural Engineers, Slovenia

The Concrete Institute, South Africa
KCI - Korean Concrete Institute, South Korea
ACHE - Asociación Cientifico-Técnica del Hormigon Estructural, Spain
SB - Svenska Betongföreningen, Sweden
Délégation nationale suisse de la *fib*, Switzerland
TCA - Thailand Concrete Association
ITU - Istanbul Technical University, Turkey
NIISK - Research Institute of Building Constructions, Ukraine
Society of Engineers, United Arab Emirates
fib UK, United Kingdom
ASBI - American Segmental Bridge Institute, United States of America
PCI - Precast/Prestressed Concrete Institute, United States of America
PTI - Post-Tensioning Institute, United States of America

Sponsoring members

Strong Force-MGC W.L.L., Bahrain
Liuzhou OVM Machinery Company, China
Shenzhen University, China
Peikko Group Corp., Finland
Consolis, France
ECS - European Engineered Construction Systems Association, Germany
FBF - Betondienst, Germany
ISB - Institut für Stahlbetonbewehrung, Germany
MKT - Metall-Kunststoff-Technik, Germany
Progress Group GmbH, Germany
Larsen & Toubro Ltd, ECC Division, India
FUJI P. S. Corporation, Japan
IHI Construction Service Company, Japan
Oriental Shiraishi Corporation, Japan
P. S. Mitsubishi Construction Company, Japan
SE Corporation, Japan
Sumitomo Mitsui Construction Company, Civil Engineering Division, Japan
Cimenterie Nationale S.A.L., Lebanon
Hilti, Liechtenstein
BBR VT International, Switzerland
Sika Schweiz, Switzerland
VSL International, Switzerland
PBL Group, Thailand
CEG – The Consulting Engineers Group, United States of America

fib Bulletins published since 1998

1 *Structural Concrete – Textbook on Behaviour, Design and Performance*; Vol. 1: *Introduction, Design Process, Materials*
Manual - textbook (244 pages, ISBN 978-2-88394-041-3, July 1999)

2 *Structural Concrete – Textbook on Behaviour, Design and Performance*; Vol. 2: *Basis of Design*
Manual - textbook (324 pages, ISBN 978-2-88394-042-0, July 1999)

3 *Structural Concrete – Textbook on Behaviour, Design and Performance*; Vol. 3: *Durability, Design for Fire Resistance; Member Design, Maintenance; Assessment and Repair, Practical aspects*
Manual - textbook (292 pages, ISBN 978-2-88394-043-7, December 1999)

4 *Lightweight aggregate concrete: Extracts from codes and standards*
State-of-the-art report (46 pages, ISBN 978-2-88394-044-4, August 1999)

5 *Protective systems against hazards: Nature and extent of the problem*
Technical report (64 pages, ISBN 978-2-88394-045-1, October 1999)

6 *Special design considerations for precast prestressed hollow core floors*
Guide to good practice (180 pages, ISBN 978-2-88394-046-8, January 2000)

7 *Corrugated plastic ducts for internal bonded post-tensioning*
Technical report (50 pages, ISBN 978-2-88394-047-5, January 2000)

8 *Lightweight aggregate concrete*: Part 1 (guide) – *Recommended extensions to Model Code 90*; Part 2 (technical report) – *Identification of research needs*; Part 3 (state-of-art report) – *Application of lightweight aggregate concrete* (118 pages, ISBN 978-2-88394-048-2, May 2000)

9 *Guidance for good bridge design*: Part 1 – Introduction, Part 2 – *Design and construction aspects*
Guide to good practice (190 pages, ISBN 978-2-88394-049-9, July 2000)

10 *Bond of reinforcement in concrete*
State-of-art report (434 pages, ISBN 978-2-88394-050-5, August 2000)

11 *Factory applied corrosion protection of prestressing steel*
State-of-art report (20 pages, ISBN 978-2-88394-051-2, January 2001)

12 *Punching of structural concrete slabs*
Technical report (314 pages, ISBN 978-2-88394-052-9, August 2001)

13 *Nuclear containments*
State-of-art report (130 pages, 1 CD, ISBN 978-2-88394-053-6, September 2001)

14 *Externally bonded FRP reinforcement for RC structures*
Technical report (138 pages, ISBN 978-2-88394-054-3, October 2001)

15 *Durability of post-tensioning tendons*
Technical report (284 pages, ISBN 978-2-88394-055-0, November 2001)

16 *Design Examples for the 1996 FIP recommendations Practical design of structural concrete*
Technical report (198 pages, ISBN 978-2-88394-056-7, January 2002)

17 *Management, maintenance and strengthening of concrete structures*
Technical report (180 pages, ISBN 978-2-88394-057-4, April 2002)

18 *Recycling of offshore concrete structures*
State-of-art report (33 pages, ISBN 978-2-88394-058-1, April 2002)

19 *Precast concrete in mixed construction*
State-of-art report (68 pages, ISBN 978-2-88394-059-8, April 2002)

20 *Grouting of tendons in prestressed concrete*
Guide to good practice (52 pages, ISBN 978-2-88394-060-4, July 2002)

21 *Environmental issues in prefabrication*
State-of-art report (56 pages, ISBN 978-2-88394-061-1, March 2003)

22 *Monitoring and safety evaluation of existing concrete structures*
State-of-art report (304 pages, ISBN 978-2-88394-062-8, May 2003)

23 *Environmental effects of concrete*
State-of-art report (68 pages, ISBN 978-2-88394-063-5, June 2003)

24 *Seismic assessment and retrofit of reinforced concrete buildings*
State-of-art report (312 pages, ISBN 978-2-88394-064-2, August 2003)

25 *Displacement-based seismic design of reinforced concrete buildings*
State-of-art report (196 pages, ISBN 978-2-88394-065-9, August 2003)

26 *Influence of material and processing on stress corrosion cracking of prestressing steel – case studies*
Technical report (44 pages, ISBN 978-2-88394-066-6, October 2003)

27 *Seismic design of precast concrete building structures*
State-of-art report (262 pages, ISBN 978-2-88394-067-3, October 2003)

28 *Environmental design*
State-of-art report (86 pages, ISBN 978-2-88394-068-0, February 2004)

29 *Precast concrete bridges*
State-of-art report (83 pages, ISBN 978-2-88394-069-7, November 2004)

30 *Acceptance of stay cable systems using prestressing steels*
Recommendation (80 pages, ISBN 978-2-88394-070-3, January 2005)

31 *Post-tensioning in buildings*
Technical report (116 pages, ISBN 978-2-88394-071-0, February 2005)

32 *Guidelines for the design of footbridges*
Guide to good practice (160 pages, ISBN 978-2-88394-072-7, November 2005)

33 *Durability of post-tensioning tendons*
Recommendation (74 pages, ISBN 978-2-88394-073-4, December 2005)

34 *Model Code for Service Life Design*
Model Code (116 pages, ISBN 978-2-88394-074-1, February 2006)

35 *Retrofitting of concrete structures by externally bonded FRPs*
Technical Report (224 pages, ISBN 978-2-88394-075-8, April 2006)

36 *2006 fib Awards for Outstanding Concrete Structures*
Bulletin (40 pages, ISBN 978-2-88394-076-5, May 2006)

37 *Precast concrete railway track systems*
State-of-art report (38 pages, ISBN 978-2-88394-077-2, September 2006)

38 *Fire design of concrete structures – materials, structures and modelling*
State-of-art report (106 pages, ISBN 978-2-88394-078-9, April 2007)

39 *Seismic bridge design and retrofit – structural solutions*
State-of-art report (300 pages, ISBN 978-2-88394-079-6, May 2007)

40 *FRP reinforcement in RC structures*
Technical report (160 pages, ISBN 978-2-88394-080-2, September 2007)

41 *Treatment of imperfections in precast structural elements*
State-of-art report (74 pages, ISBN 978-2-88394-081-9, November 2007)

42 *Constitutive modelling of high strength / high performance concrete*
State-of-art report (130 pages, ISBN 978-2-88394-082-6, January 2008)

43 *Structural connections for precast concrete buildings*
Guide to good practice (370 pages, ISBN 978-2-88394-083-3, February 2008)

44 *Concrete structure management: Guide to ownership and good practice*
Guide to good practice (208 pages, ISBN 978-2-88394-084-0, February 2008)

45 *Practitioners' guide to finite element modelling of reinforced concrete structures*
State-of-art report (344 pages, ISBN 978-2-88394-085-7, June 2008)

46 *Fire design of concrete structures —structural behaviour and assessment*
State-of-art report (214 pages, ISBN 978-2-88394-086-4, July 2008)

47 *Environmental design of concrete structures – general principles*
Technical report (48 pages, ISBN 978-2-88394-087-1, August 2008)

48 *Formwork and falsework for heavy construction*
Guide to good practice (96 pages, ISBN 978-2-88394-088-8, January 2009)

49 *Corrosion protection for reinforcing steels*
Technical report (122 pages, ISBN 978-2-88394-089-5, February 2009)

50 *Concrete structures for oil and gas fields in hostile marine environments*
State-of-art report (36 pages, IBSN 978-2-88394-090-1, October 2009)

51 *Structural Concrete – Textbook on behaviour, design and performance*, Vol. 1
Manual – textbook (304 pages, ISBN 978-2-88394-091-8, November 2009)

52 *Structural Concrete – Textbook on behaviour, design and performance*, Vol. 2
Manual – textbook (350 pages, ISBN 978-2-88394-092-5, January 2010)

53 *Structural Concrete – Textbook on behaviour, design and performance*, Vol. 3
Manual – textbook (390 pages, ISBN 978-2-88394-093-2, December 2009)

54 *Structural Concrete – Textbook on behaviour, design and performance*, Vol. 4
Manual – textbook (196 pages, ISBN 978-2-88394-094-9, October 2010)

55 *fib Model Code 2010, First complete draft* – Volume 1
Draft Model Code (318 pages, ISBN 978-2-88394-095-6, March 2010)

56 *fib Model Code 2010, First complete draft* – Volume 2
Draft Model Code (312 pages, ISBN 978-2-88394-096-3, April 2010)

57 *Shear and punching shear in RC and FRC elements - Workshop proceedings*
Technical report (268 pages, ISBN 978-2-88394-097-0, October 2010)

58 *Design of anchorages in concrete*
Guide to good practice (282 pages, ISBN 978-2-88394-098-7, July 2011)

59 *Condition control and assessment of reinforced concrete structures exposed to corrosive environments (carbonation/chlorides)*
State-of-art report (80 pages, ISBN 978-2-88394-099-4, May 2011)

60 *Prefabrication for affordable housing*
State-of-art report (130 pages, ISBN 978-2-88394-100-7, August 2011)

61 *Design examples for strut-and-tie models*
Technical report (220 pages, ISBN 978-2-88394-101-4, September 2011)

62 *Structural Concrete – Textbook on behaviour, design and performance*, Vol. 5
Manual – textbook (476 pages, ISBN 978-2-88394-102-1, January 2012)

63 *Design of precast concrete structures against accidental actions*
Guide to good practice (78 pages, ISBN 978-2-88394-103-8, January 2012)

64 *Effect of zinc on prestressing steel*
Technical report (22 pages, ISBN 978-2-88394-104-5, February 2012)

65 *fib Model Code 2010*, Final draft – Volume 1
Model Code (350 pages, ISBN 978-2-88394-105-2, March 2012)

66 *fib Model Code 2010*, Final draft – Volume 2
Model Code (370 pages, ISBN 978-2-88394-106-9, April 2012)

67 *Guidelines for green concrete structures*
Guide to good practice (56 pages, ISBN 978-2-88394-107-6, May 2012)

68 *Probabilistic performance-based seismic design*
Technical report (118 pages, ISBN 978-2-88394-108-3, July 2012)

69 *Critical comparison of major seismic codes for buildings*
Technical report (216 pages, ISBN 978-2-88394-109-0, August 2013)

70 *Code-type models for structural behaviour of concrete*
State-of-art report (196 pages, ISBN 978-2-88394-110-6, November 2013)

71 *Integrated life cycle assessment of concrete structures*
State-of-art report (62 pages, ISBN 978-2-88394-111-3, December 2013)

72 *Bond and anchorage of embedded reinforcement: Background to the fib Model Code for Concrete Structures 2010*
Technical report (170 pages, ISBN 978-2-88394-112-0, May 2014)

73 *Tall buildings: Structural design of concrete buildings up to 300m tall*
State-of-the-art report (158) pages, ISBN 978-2-88394-113-7, August 2014)

74 *Planning and design handbook on precast building structures*
Manual – textbook (313 pages, ISBN 978-2-88394-114-4, September 2014)

75 *Polymer-duct systems for internal bonded post-tensioning*
Recommendation (172 pages, ISBN 978-2-88394-115-1, December 2014)

76 *Benchmarking of deemed-to-satisfy provisions in standards: Durability of Reinforced Concrete Structures Exposed to Chlorides*
State-of-the-art-report (191 pages, ISBN 978-2-88394-116-8, May 2015)

77 *Corrugated-steel-web bridges*
State-of-the-art-report (110 pages, ISBN 978-2-88394-117-5, December 2015)

78 *Precast-concrete buildings in seismic areas*
State-of-the-art-report (273 pages, ISBN 978-2-88394-118-2, March 2016)

79 *Fibre-reinforced concrete - From design to structural applications*
ACI-*fib* workshop proceedings (480 pages, ISBN 978-2-88394-119-9, May 2016)

80 *Partial factor methods for existing concrete structures*
Recommendation (129 pages, ISBN 978-2-88394-120-5, December 2016)

81 *Punching of structural concrete slabs: Honoring Neil M. Hawkins*
ACI SP-315, ACI-*fib* symposium proceedings (378 pages, ISBN 978-2-88394-121-2, April 2017)

82 *Precast segmental bridges*
Guide to good practice (183 pages, ISBN 978-2-88394-122-9, August 2017)

83 *Precast Tunnel Segments in Fibre-Reinforced Concrete*
State-of-the-art report (162 pages, ISBN 978-2-88394-123-6, November 2017)

84 *Precast insulated sandwich panels*
State-of-the-art report (129 pages, ISBN 978-2-88394-124-3, December 2017)

85 *Towards a rational understanding of shear in beams and slabs*
Technical Report (338 pages, ISBN 978-2-88394-125-0, May 2018)

86 *Safety and performance concepts*
Guide to good practice (357 pages, ISBN 978-2-88394-126-7, August 2018)

87 *2018 fib Awards for Outstanding Concrete Structures*
Bulletin (39 pages, ISBN 978-2-88394-127-4, October 2018)

88 *Sustainability of precast structures*
State-of-the-art report (153 pages, ISBN 978-2-88394-128-1, December 2018)

89 *Acceptance of cable systems using prestressing steels*
Recommendation (153 pages, ISBN 978-2-88394-129-8, March 2019)

90 *Externally applied FRP reinforcement for concrete structures*
Technical report (229 pages, ISBN 978-2-88394-131-1, May 2019)

91 *Floating concrete structures*
State-of-the-art report (100 pages, ISBN 978-2-88394-133-5, August 2019)

92 *Serviceability Limit State of Concrete Structures*
Technical report (209 pages, ISBN 978-2-88394-135-9, September 2019)

93 *Birth Certificate and Through-Life Management Documentation*
Technical report (96 pages, ISBN 978-2-88394-137-3, June 2020)

Abstracts for *fib* Bulletins and lists of available CEB Bulletins and FIP Reports are available on the *fib* website at www.fib-international.org/publications.

fib CEB-FIP

PCI Precast/Prestressed Concrete Institute

Precast concrete bridge continuity over piers

Contents

ISBN 978-2-88394-140-3

International Federation for Structural Concrete
Fédération internationale du béton
www.fib-international.org

ISSN: 1562-3610